

https://dspace.org/

Recommendations for the reporting and interpretation of isotope dilution UPb geochronological information

D Condon; B Schoene; M Schmitz; Scott MacLennan; et al

GEOLOGICAL SOC AMER, INC
https://hdl.handle.net/10539/40981
WOS

Downloaded from a DSpace repository. https://dspace.org/

THE GEOLOGICAL SOCIETY OF AMERICA®

THEMED ISSUE: Reporting and Interpretation of Geochronologic Data

Recommendations for the reporting and interpretation of isotope dilution U-Pb geochronological information

Dan Condon[1], Blair Schoene[2,†], Mark Schmitz[3], Urs Schaltegger[4], Ryan B. Ickert[5], Yuri Amelin[6], Lars E. Augland[7], Kevin R. Chamberlain[8], Drew S. Coleman[9], James N. Connelly[10], Fernando Corfu[7], James L. Crowley[3], Joshua H.F.L. Davies[11], Steven W. Denyszyn[12], Michael P. Eddy[5], Sean P. Gaynor[2], Larry M. Heaman[13], Magdalena H. Huyskens[14], Sandra Kamo[15], Jennifer Kasbohm[16], C. Brenhin Keller[17], Scott A. MacLennan[18], Noah M. McLean[19], Stephen Noble[1], Maria Ovtcharova[4], André Paul[4], Jahandar Ramezani[20], Matt Rioux[21], Diana Sahy[1], James S. Scoates[22], Dawid Szymanowski[23], Simon Tapster[1], Marion Tichomirowa[24], Corey J. Wall[22], Jörn-Frederik Wotzlaw[23], Chuan Yang[25], and Qing-Zhu Yin[26]

[1]*British Geological Survey, Keyworth, Nottinghamshire NG12 5GG, UK*
[2]*Department of Geosciences, Princeton University, Princeton, New Jersey 08544, USA*
[3]*Department of Geosciences, Boise State University, Boise, Idaho 83725, USA*
[4]*Department of Earth Sciences, University of Geneva, 1211 Geneva, Switzerland*
[5]*Department of Earth, Atmospheric, and Planetary Sciences, Purdue University, West Lafayette, Indiana 47907, USA*
[6]*Korea Basic Science Institute, Ochang, Cheongwon, Cheongju, Chungbuk 28119, Republic of Korea*
[7]*Department of Geosciences, University of Oslo, N-0316 Oslo, Norway*
[8]*Department of Geology and Geophysics, University of Wyoming, Laramie, Wyoming 82071, USA*
[9]*Department of Earth, Marine and Environmental Sciences, University of North Carolina–Chapel Hill, Chapel Hill, North Carolina 27599, USA*
[10]*Centre for Star and Planet Formation, Globe Institute, University of Copenhagen, Øster Voldgade 5-7, DK-1350 Copenhagen, Denmark*
[11]*Département des sciences de la Terre et de l'atmosphère/Geotop, Université du Québec à Montréal, Montréal, Québec H2X 3Y7, Canada*
[12]*Department of Earth Sciences, Memorial University of Newfoundland, St. John's, Newfoundland A1C 5S7, Canada*
[13]*Department of Earth and Atmospheric Sciences, University of Alberta, Edmonton, Alberta T6G 2E3, Canada*
[14]*Norges geologiske undersøkelse (NGU), Leiv Eirikssons vei 39, 7040 Trondheim, Norway*
[15]*Department of Earth Sciences, University of Toronto, Toronto, Ontario M5S 3B1, Canada*
[16]*Department of Earth & Planetary Sciences, Yale University, New Haven, Connecticut 06520, USA*
[17]*Department of Earth Sciences, Dartmouth College, Hanover, New Hampshire 03755, USA*
[18]*School of Geosciences, University of the Witwatersrand, Johannesburg Wits 2050, South Africa*
[19]*Department of Geology, University of Kansas, Lawrence, Kansas 66045, USA*
[20]*Department of Earth, Atmospheric, and Planetary Sciences, Massachusetts Institute of Technology, Cambridge, Massachusetts 02139, USA*
[21]*Department of Earth Science, University of California, Santa Barbara, Santa Barbara, California 93106, USA*
[22]*Pacific Centre for Isotopic and Geochemical Research, Department of Earth, Ocean and Atmospheric Sciences, 2020-2207 Main Mall, University of British Columbia, Vancouver, British Columbia V6T 1Z4, Canada*
[23]*Institute of Geochemistry and Petrology, ETH Zurich, 8092 Zurich, Switzerland*
[24]*TU Bergakademie Freiberg, Institute for Mineralogy, Brennhausgasse 14, D-09596 Freiberg, Germany*
[25]*Nanjing Institute of Geology and Palaeontology, Chinese Academy of Sciences, Nanjing 210008, China*
[26]*Department of Earth and Planetary Sciences, University of California, Davis, Davis, California 95616, USA*

ABSTRACT

U-Pb geochronology by isotope dilution–thermal ionization mass spectrometry (ID-TIMS) has the potential to be the most precise and accurate of the deep time chronometers, especially when applied to high-U minerals such as zircon. Continued analytical improvements have made this technique capable of regularly achieving better than 0.1% precision and accuracy of dates from commonly occurring high-U minerals across a wide range of geological ages and settings. To help maximize the long-term utility of published results, we present and discuss some recommendations for reporting ID-TIMS U-Pb geochronological data and associated metadata in accordance with accepted principles of data management. Further, given that the accuracy of reported ages typically depends on the interpretation applied to a set of individual dates, we discuss strategies for data

Blair Schoene https://orcid.org/0000-0001-7092-8590
†bschoene@princeton.edu

GSA Bulletin; September/October 2024; v. 136; no. 9/10; p. 4233–4251; https://doi.org/10.1130/B37321.1.
Published online 1 April 2024

© 2024 The Authors. Gold Open Access:
This paper is published under the terms of the CC-BY license.

Downloaded from http://pubs.geoscienceworld.org/gsa/gsabulletin/article-pdf/136/9-10/4233/6898541/b37321.1.pdf
by guest

interpretation. We anticipate that this paper will serve as an instructive guide for geologists who are publishing ID-TIMS U-Pb data, for laboratories generating the data, the wider geoscience community who use such data, and also editors of journals who wish to be informed about community standards. Combined, our recommendations should increase the utility, veracity, versatility, and "half-life" of ID-TIMS U-Pb geochronological data.

1. INTRODUCTION

U-Pb geochronology is used to date commonly occurring U-bearing minerals for inferring the ages of geological materials and processes in a wide range of environments across Earth history (e.g., the Geologic Time Scale 2020; Davis et al., 2003; Mattinson, 2013; Schoene, 2014). The decay of ^{238}U and ^{235}U ($t_{1/2}$ ^{238}U, ca. 4.47 Ga; ^{235}U, ca. 0.704 Ga) to their stable daughter products, ^{206}Pb and ^{207}Pb, respectively, can be determined in minerals with ages ranging from ca. 100 ka to the age of the Solar System. Among the techniques presently used to measure the parent and daughter ratios, the most precise and accurate approach is by isotope dilution–isotope ratio mass spectrometry (ID-IRMS), usually via thermal ionization mass spectrometry (TIMS; Parrish and Noble, 2003; Tilton et al., 1955a). Note that we use the term ID-TIMS throughout this manuscript, but that some labs (see main text) measure U by multicollector–inductively coupled plasma–mass spectrometry (MC-ICP-MS). This may become increasingly popular in the future, but currently the methods and applications described in this paper are equated with what geologists and geochemists recognize as "(CA)-ID-TIMS U-Pb" geochronology, so we use this term, which may be more aptly referred to as (CA)-ID-IRMS (where IR is isotope ratio) geochronology.

Innovations in ID-TIMS U-Pb geochronology over the past few decades include more precise and accurate mass spectrometry, increasingly rigorous and cleaner sample preparation, more transparent data treatment and assessment of uncertainties, calibration to the International System of Units (SI), interlaboratory standardization, and more informed interpretations of how dates calculated correspond to the age of a geological event. Additionally, more thorough sample characterization through complementary analytical techniques has provided more geologically reasonable interpretations of dates in a petrologic context (Kohn et al., 2017). To best capitalize on these advances, however, several issues need to be addressed. Firstly, to meaningfully compare different high-precision data sets, assessment of interlaboratory reproducibility and bias must be addressed (Schaltegger et al., 2021). In addition to carefully planned interlaboratory experiments on reference materials, addressing interlaboratory analytical bias requires reporting U-Pb data from mineral and/or solution reference materials along with sample data in each study. Secondly, it must be acknowledged that the accuracy of an age depends on the robustness of the interpretations of how a date corresponds to a geologic process or event. For example, an eruption age for an ash bed based on U-Pb zircon dates may require interpretation of a potentially complex data set that includes zircon dates that predate eruption (Galeotti et al., 2019; Griffis et al., 2019; Keller et al., 2018; Ovtcharova et al., 2015; Sahy et al., 2017). Indeed, increased precision of ID-TIMS U-Pb data has led to a situation in which different approaches to inferring a geologic process (such as eruption) from a complicated data set can result in different high-precision age interpretations from the same data set. To tackle both concerns, complete data sets must be presented along with available metadata to provide adequate information for a broader community that wants to incorporate those data into their work, and to give researchers the ability to produce and assess alternative age interpretations based upon those data.

Toward these ends, this paper outlines data reporting requirements for U-Pb geochronology by ID-TIMS, followed by a discussion of salient issues related to data interpretation and age assignments. We cover three main areas: (1) data reporting, to provide a guide for users, authors, reviewers, and editors that outlines the information required for the publication of ID-TIMS U-Pb data, as well as some suggestions about useful data and metadata that should be reported for quality control and the ability to assess interlaboratory bias; (2) data interpretation, to provide guidance for the interpretation of data sets to derive geologically significant ages, and for users to understand how data interpretation results in reported dates; and (3) current state-of-the-art approaches in ID-TIMS U-Pb geochronology, including its combination with a range of microanalytical techniques that lead to richer and more accurate age interpretations. We have attempted to minimize the bias toward the discussion of issues related to U-Pb zircon dating, although this accounts for the majority of U-Pb data being published. Regardless, we define criteria for data reporting in a way that is applicable to all minerals used for U-Pb dating. Also, although this contribution is focused on ID-TIMS U-Pb geochronology, many of the points for discussion are generic and can be applied to a wide range of radioisotopic dating and tracing.

2. BACKGROUND ON ISOTOPE DILUTION U-Pb GEOCHRONOLOGY

U-Pb geochronology is applied to U-bearing minerals that form in a range of magmatic, metamorphic, and (to a lesser extent) sedimentary and hydrothermal environments. The method benefits from the key attributes of the U-Pb decay scheme, namely the dual decay of U (^{238}U decays to ^{206}Pb, and ^{235}U decays to ^{207}Pb), which provides an internal check on open/closed system behavior via concordance of the two decay schemes. Zircon ($ZrSiO_4$), in particular, is extremely well suited to U-Pb geochronology as it preferentially incorporates U^{4+} into its crystal lattice during crystallization but excludes Pb^{2+}. This is also true for baddeleyite (ZrO_2), which has become a cornerstone for interpreting the age of mafic magmatism. This means that the correction for initial daughter isotopes in the age equation is minimized, improving a date's precision and accuracy. Other moderate- to high-U minerals include monazite, titanite, and rutile. Perovskite and apatite can contain appreciable amounts of initial Pb upon crystallization, but because this can be tracked using the nonradiogenic ^{204}Pb content in ID-TIMS analyses, accurate corrections can be made for initial Pb using a variety of approaches, but always at the cost of precision (Chamberlain and Bowring, 2001; Ludwig, 1998; Schmitz and Bowring, 2001).

U-Pb geochronology by ID-TIMS requires dissolving minerals in acids, chemically separating U and Pb from the other elements in the mineral using anion exchange chemistry, and measuring the ratios of U and Pb isotopes by mass spectrometry. To account for potential loss of either U or Pb during the chemical separation process and differences in ionization during mass spectrometric analyses, it is necessary to add an isotopic tracer to the sample to determine an accurate inter-element (U/Pb) ratio. This process, called isotope dilution (ID; Inghram, 1954; Stracke et al., 2014; Webster, 1959), involves mixing a sample with a solution containing a known amount/ratio of purified parent and daughter isotopes prior to dissolving the mineral. In the case of modern U-Pb ID-TIMS analyses, the tracer contains enriched abundances of naturally occurring and/or synthetically produced isotopes of both U and Pb (e.g., ^{202}Pb, ^{205}Pb, ^{233}U, and ^{236}U) whose ratios are carefully calibrated (Condon et al., 2015; McLean et al., 2015). If the isotope tracer contains at least one unnaturally occurring isotope of both U and Pb and its isotopic composition is known, the U and Pb isotope ratio measurements of the homogenized tracer-sample mixture are the only requirements for determining the mass of isotopes of interest in the sample. The abundances of the tracer isotopes are determined by calibra-

Downloaded from http://pubs.geoscienceworld.org/gsa/gsabulletin/article-pdf/136/9-10/4233/6898541/b37321.1.pdf
by guest

tion against gravimetrically determined solutions (i.e., solutions of determined isotopic compositions whose elemental concentrations are known via weighing), so isotope dilution measurements of samples can be directly traced to the SI unit of the kilogram (Condon et al., 2015; Wasserburg et al., 1981). This makes it a so-called "primary" measurement technique whereby U/Pb ratios can be traced back to SI units. When combined with the determination of the ^{238}U and ^{235}U decay constants (Jaffey et al., 1971), U-Pb dates are more confidently thought to accurately quantify geologic time.

U-Pb determinations by ID-TIMS are also increasingly important for the accuracy of standard-bracketed U-Pb methods and other radioisotope systems used for geochronology. For example, microbeam U-Pb methods such as laser ablation–inductively coupled plasma–mass spectrometry (LA-ICP-MS) and secondary ion mass spectrometry (SIMS) determine U/Pb ratios relative to a reference material whose U/Pb is known via ID methods (Schaltegger et al., 2015; Stracke et al., 2014; Williams, 1998). Furthermore, decay constants used in other radioisotopic dating methods (e.g., Rb-Sr, ^{40}Ar/^{39}Ar, and Re-Os) have been intercalibrated with U-Pb dates from the same geological materials (Nebel et al., 2010; Renne et al., 2010; Selby et al., 2007). As intercalibration experiments continue to improve, the accuracy of ID-TIMS U-Pb geochronology will be incorporated into other geochronological methods.

Critical for further improving the precision and accuracy of U-Pb dates is the availability of suitable U and Pb isotopic tracers and the precise and accurate knowledge of their isotopic composition. In the first decades of ID-TIMS U-Pb geochronology, tracers were mainly composed of enriched ^{208}Pb, ^{235}U, and ^{230}Th (Krogh, 1973; Tilton et al., 1955b). The production of a ^{205}Pb tracer (Krogh and Davis, 1975; Newman et al., 1976; Parrish and Krogh, 1987) and to a lesser extent ^{202}Pb (Todt et al., 1996) allowed measurements of Pb isotope compositions and abundances to be made on the same aliquot. The later addition of synthetic ^{233}U and/or ^{236}U tracers in addition to, or in lieu of ^{235}U, allowed for a more accurate and precise correction for instrumental mass bias (Richter et al., 2008). U-Pb geochronology via ID-TIMS using a double-Pb, double-U tracer is capable of producing U-Pb dates of minerals such as zircon with uncertainties of <0.05% (Nasdala et al., 2018; Szymanowski and Schoene, 2020). For U-Pb dates to also be demonstrably accurate at the 0.05% level, transparency in data generation, reduction, reporting, and interpretation needs to be consistent across the literature. The rest of this paper is focused on recommendations that will help achieve this goal.

3. DATA AND METADATA REPORTING

Recommendations for data reporting associated with ID-TIMS U-Pb geochronology are aimed at aiding the interoperability and reusability of U-Pb geochronological data. We differentiate the term "date"—the number calculated using the decay equation or through a statistical interpretation such as a weighted mean or isochron (Section 6)—from "age," which applies an interpretation to dates and therefore adds geologic significance. Although it is uncommon in the literature to report either dates or ages without analytical data, the underlying analytical data, rather than simply age interpretations, are required for the following reasons:

(1) *To facilitate the reproduction of a set of U-Pb dates.* The dates from which an age is derived are calculated based upon a number of input parameters, some of which are measured for a specific mineral (e.g., isotope ratios), some of which are estimated for a sample or group of samples (e.g., an analytical blank contribution), and some of which are common to all samples and often referred to as "constants" (e.g., a decay constant). When calculations that convert isotope ratios to radioisotopic dates require reassessment (e.g., ^{230}Th disequilibrium correction, Section 3.3), the appropriate input parameters are necessary; therefore, they should be published with the data.

(2) *To evaluate the quality of a set of U-Pb dates.* Enough data and metadata should be reported for a reader to assess the quality of U-Pb dates. These include attributes such as the ratio of radiogenic to common Pb, which should scale with uncertainty in the resulting dates in most cases (Schoene and Baxter, 2017); noncorrelation could imply issues with mass spectrometry. These also include data for U-Pb reference materials that allow assessment of intralaboratory and interlaboratory reproducibility.

(3) *To enhance the longevity of a set of U-Pb dates.* Constant values and uncertainties that apply to all data sets (e.g., decay constants and sample ^{238}U/^{235}U) are estimated based upon experimental data such that new values can be determined periodically. Capturing the appropriate levels of data and metadata allows legacy data to be updated using different input values, thus extending the useful life of the sample data.

(4) *To allow (re)examination of the derived age interpretations based upon sets of U-Pb dates.* Proper documentation of the data and metadata underlying U-Pb dates will allow others to derive alternative age (and/or uncertainty) interpretation(s) for a given mineral or sample.

In the following paragraphs we propose a list of data, metadata, parameters, and constants that provide a sufficient description of the data set to meet the broad goals described above, which we consider to be required for publication. The workflow is presented in Figure 1 with identical header and subheader numbering in the text. We note that some of these procedures are quite standard, and in such cases, it may be sufficient to reference a publication with the complete workflow or process described. Figure 1 can also be used as a checklist for those wishing to confirm that both necessary and optional data reporting guidelines are met.

3.1. Sample Characterization

3.1.1. Sample Collection

Sample metadata such as location and geological context commonly reside in the narrative of a publication, as well as within data tables and figures. Samples should be provided with a unique geographical identifier that is associated with metadata about the nature of the sample (see below). The location description must be sufficient for sampling to be reproduced. This is highly sample-specific and may include Universal Transverse Mercator (UTM) or latitude–longitude coordinates (at a precision sufficient to reproduce the sampling locality), site descriptions, stratigraphic sections, borehole logs, and/or (micro-)photographs. Authors should consider linking sample metadata to a persistent, unique, and actionable registered sample identification number such as an International Generic Sample Number (IGSN) that can be provided by the SESAR System for Earth Sample Registration.

3.1.2. Mineral Location and Separation

Indicate whether minerals were obtained through bulk or selective sampling, and whether selection was preceded by petrographic contextualization. If the materials analyzed are separated from a rock sample, the separation process should be described, and the host rock should be described in sufficient detail to understand the relationship of the separated mineral to the host, to be able to interpret eventual chemical data obtained from the dated material, and to relate the host to the geologic phenomena under consideration.

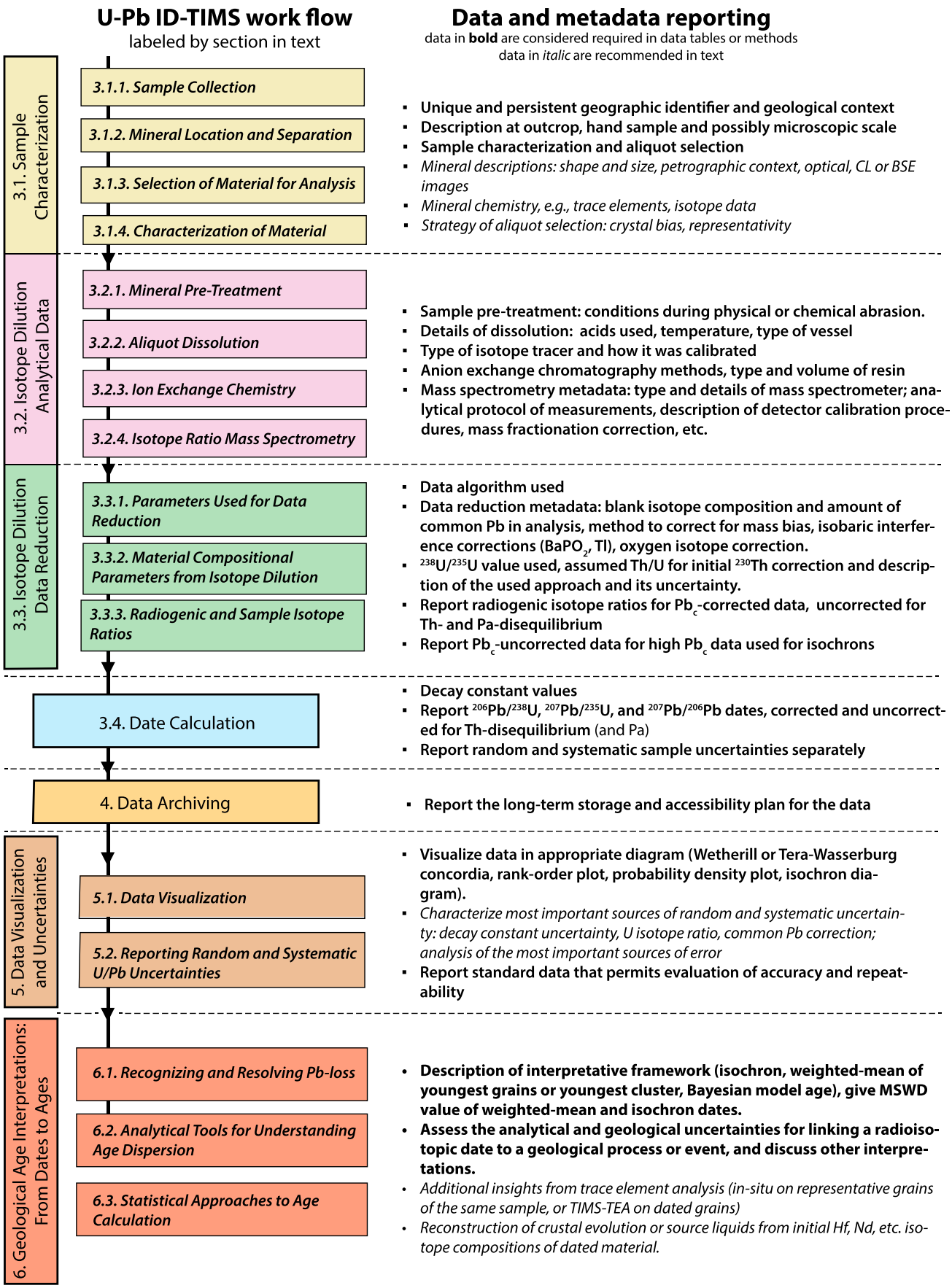
3.1.3. Selection of Material for Analysis

Describe the criteria that guided the selection of the material analyzed (i.e., minerals chosen) from the bulk mineral concentrate.

3.1.4. Characterization of the Material Dated

Samples analyzed should be described with sufficient detail to understand the nature of the material being measured. Information about the size, shape, color, consistency, and quality (e.g., presence of mineral/fluid inclusions, alteration, zoning, fractures, etc.) of the grains is important

Downloaded from http://pubs.geoscienceworld.org/gsa/gsabulletin/article-pdf/136/9-10/4233/6898541/b37321.1.pdf
by guest



Downloaded from http://pubs.geoscienceworld.org/gsa/gsabulletin/article-pdf/136/9-10/4233/6898541/b37321.1.pdf
by guest

Figure 1. Schematic workflow diagram for U-Pb geochronology by chemical abrasion–isotope dilution–thermal ionization mass spectrometry (CA-ID-TIMS). Left side of diagram outlines workflow with sections of text labeled. Refer to those sections for more detail. Right side of diagram lists, in brief, data and metadata required and recommended for reporting in studies containing ID-TIMS U-Pb data. This list can be used as a checklist for those evaluating data reporting in their own or other papers. Each item on the list is discussed in more detail in related sections of the text. BSE—backscattered electron; CL—cathodoluminescence; TIMS-TEA—thermal ionization mass spectrometry–trace element analysis.

for a proper interpretation of the U-Pb results and dates. Were the samples analyzed comprised of multiple grains, single crystals, or crystal fragments? Optical, cathodoluminescence (CL), backscattered electron (BSE) images, and/or X-ray maps are desirable for understanding mineral textures, petrographic settings, morphologies, and petrogenesis. Screening zircon grains using micro-Raman spectrometry can inform about the degree of decay damage and quantify the success of the chemical abrasion treatment (McKanna et al., 2023; McKanna et al., 2024; Widmann et al., 2019). In situ U-Pb methods can be used to characterize age populations for given minerals, or U/Pb variation in initial Pb-bearing phases, to aid in the selection of material for ID-TIMS analyses. Dated grains that were imaged prior to analysis should be identified, so the reader can connect a date to the image of the mineral, and it can be beneficial to include complementary trace element or isotopic data (e.g., Hf, O, Li, etc.) from minerals analyzed for geochronology. These analyses can be conducted in situ prior to ID-TIMS using electron probe microanalysis (EPMA), LA-ICP-MS, or SIMS techniques (Chelle-Michou et al., 2014; Rivera et al., 2014; Samperton et al., 2015; Wall et al., 2021), or on the material left over from chemical purification after mineral dissolution through solution ICP-MS (Amelin et al., 1999; Schoene et al., 2010b). While we do not make specific recommendations here for these other analytical methods, these data and analytical protocols should also be published with adequate detail, as dictated by those methods, to meet the same goals targeted by the recommendations for U-Pb data in this paper.

3.2. Isotope Dilution Analytical Data

The analytical data should be reported in the methods section and/or a data table (Tables S1 and S2 in the Supplemental Material[1]) and also stored using a unique sample identifier in a publicly accessible data archive (see Section 4). In the following text, an asterisk, such as Pb*, refers to the radiogenic daughter product, a subscript "c," such as Pb_c, refers to "common" or nonradiogenic Pb present when the mineral crystallized (referred to below as initial Pb) plus that introduced as blank during laboratory work (referred to as blank Pb). Given relatively consistent blank Pb values, the term "high Pb_c minerals" used below refers to those with high initial Pb. Data tables should be provided in a form that is easily machine-readable. Annotated examples of data tables are included (Table S1 provides an example for a mineral with high Pb^*/Pb_c, such as zircon; see Table S2 for a mineral with low Pb^*/Pb_c, such as apatite).

3.2.1. Mineral Pre-Treatment

Has the sample undergone any pre-treatment to minimize the impact of Pb-loss (mechanical or chemical abrasion) or surface contamination? If the chemical abrasion method (Mattinson, 2005) was applied (and it generally should be for zircon), report duration and temperature of both annealing and partial dissolution steps, as well as the concentration of the acids (e.g., Huyskens et al., 2016; Mattinson, 2005; McKanna et al., 2023; McKanna et al., 2024; Widmann et al., 2019).

3.2.2. Aliquot Dissolution

Report conditions of dissolution such as type of dissolution vessel, temperature, duration, acid strength, and whether and how complete dissolution was verified. This step typically begins with the addition of the isotope tracer to the sample; verifying sample dissolution facilitates assessment of sample/tracer homogenization. Report which U-Pb tracer was used and how it was calibrated (e.g., reference a paper that outlines the calibration; Condon et al., 2015; McLean et al., 2015).

3.2.3. Ion Exchange Chemistry

If ion exchange chemistry was employed to purify U and Pb, describe the size and volume of columns and the type of resin. Briefly describing the entire separation protocol, including acid molarities and volumes, is desirable but not required. When standard approaches are employed, a publication that describes these can be referenced.

3.2.4. Isotope Ratio Mass Spectrometry

Indicate which mass spectrometer was used for isotope ratio analysis, and how the isotope ratios for each element were measured. While most labs use TIMS to measure uranium as the oxide, some labs measure uranium as the metal either by TIMS or MC-ICP-MS (Liao et al., 2020; Tissot and Dauphas, 2015; Zhou et al., 2019); in either case, it is important to indicate the type and maker of the mass spectrometer, in addition to various calibration protocols. For example, a study should indicate whether ion counting, faraday only, or combined faraday-ion counting mode was employed. Static or dynamic multicollector modes versus dynamic single-collector modes should also be indicated. How were the ion counting parameters such as deadtime and detector linearity calibrated and verified? How were faraday cup efficiencies and gains determined, what signal amplification technology was used, and what integration times were used and how were tau corrections applied? Indicate the type of loading solution that was used on filaments (e.g., Si-gel or silicic acid; Gerstenberger and Haase, 1997). Due to corrections described below that are applied to raw ion counts or currents, these are not recommended for reporting.

3.3. Isotope Dilution Data Reduction

Following mass spectrometry, the measured isotope ratios are corrected for a number of factors related to the measurement itself (e.g., mass-dependent fractionation), and also for subtraction of nonradiogenic isotopes (e.g., initial and blank Pb, and tracer isotopes). The end result of this permits calculation of the isotope ratios and compositional parameters reported in example Tables S1 and S2.

3.3.1. Parameters Used for Data Reduction

In the methods section, it is important to report which software was used for isotope ratio data visualization and discrimination (e.g., Bowring et al., 2011) and which algorithm and/or software was used for data reduction (e.g.,

[1]Supplemental Material. Table 1: Example data table for U-Pb CA-ID-TIMS isotopic data for a mineral low in common Pb. Table 2: U-Pb ID-TIMS isotopic data for a single mineral grain high in common Pb. Please visit https://doi.org/10.1130/GSAB.S.25308946 to access the supplemental material, and contact editing@geosociety.org with any questions.

Downloaded from http://pubs.geoscienceworld.org/gsa/gsabulletin/article-pdf/136/9-10/4233/6898541/b37321.1.pdf
by guest

McLean et al., 2011; Schmitz and Schoene, 2007). Typical practice is to report the amounts and isotopic composition of laboratory Pb and U blank (typically a mass), their uncertainties, and how these were estimated (Tables S1 and S2). In addition, the isotopic composition (and uncertainties) used to subtract both blank and initial common Pb from the total Pb budget must be reported, with a statement about how these values were determined. Was the ratio of $^{238}U/^{235}U$ in the sample measured directly on the aliquot dated (Tissot et al., 2019) or was an assumed value based upon $^{238}U/^{235}U$ studies on other U-bearing minerals (Hiess et al., 2012)? The approach to correction for mass bias during mass spectrometry needs to be outlined (e.g., "power-law," etc.). For example, were the mass bias corrections based on external measurements of standard materials (e.g., SRM 981), or on internal double spike (e.g., ^{202}Pb-^{205}Pb) measurements? Were molecular or isobaric interferences monitored and/or corrected for (e.g., masses 201 and 204 for $BaPO_2$ and 203 and 205 for Tl interferences), and if a correction was done, what isotopic composition (e.g., $^{203}Tl/^{205}Tl$) was used for the interfering species? Measurement of U as UO_2 is a common practice with TIMS, and reporting of the $^{18}O/^{16}O$ forming the oxide as well as the uncertainty used are required. If an $^{18}O/^{16}O$ value was used based upon an assumed "natural" value, report the value and a reference; if measured directly during the ID-TIMS analyses (Szymanowski and Schoene, 2020) or inferred based on other measurements using the same analytical setup (Condon et al., 2015), describe the analytical approach.

3.3.2. Material Compositional Parameters from Isotope Dilution

ID-TIMS permits the determination of the absolute amount of U and Pb in a given aliquot given the known tracer isotope concentration and amount of tracer added. Typical practice is to report the mass of radiogenic Pb (Pb*), the mass of common Pb (Pb_c), and their ratio. The $^{206}Pb/^{204}Pb$ ratio (corrected for mass fractionation and tracer Pb contributions, but not blank and initial Pb contents; reported in isotope ratios in Table S1) has been reported historically as a measure of the ratio of radiogenic to common Pb in the analysis, and serves as a proxy of radiogenic to common Pb for a $^{206}Pb/^{238}U$ date. In many ways it is redundant to the required Pb^*/Pb_c parameter, which seems to be what many analysts prefer to see. Notably, the Pb^*/Pb_c is usually calculated including $^{208}Pb^*$, which means that for U-Pb geochronology of high Th/U minerals (e.g., monazite, perovskite, and titanite), the Pb^*/Pb_c may not correlate well with the uncertainty on the $^{206}Pb/^{238}U$ date, but the $^{206}Pb/^{204}Pb$ does.

Molar quantities of Pb and U, combined with a mass or volume estimate, permit the calculation of the U and Pb concentrations in the aliquot. At present, the sample sizes of single mineral grains (<10 μg) are too small for weighing to be practical, but volumes may be estimated from photographs. More recently, removal of material during chemical abrasion (Mattinson, 2005) has added further uncertainty to the post-leached volume or mass (however, see McKanna et al., 2023). For these reasons, we place U and Pb concentrations in the recommended rather than required category, and they are not shown in Tables S1 and S2. However, reporting the sample U mass (in pg or ng) will allow possible inaccuracies due to insufficient U available for measurement to be evaluated, and we recommend that it be reported.

The Th/U ratio of an analyzed mineral is calculated based upon the $^{208}Pb^*/^{206}Pb^*$ ratio in the aliquot, a nominal age (from the U-Pb system), and the Th and U decay constants; this is required for estimation and correction of initial ^{230}Th disequilibrium (Parrish, 1990; Schärer, 1984). Figures 2D and 3D illustrate the magnitude and direction of this bias on $^{206}Pb/^{238}U$ dates. Reporting of the $^{208}Pb^*/^{206}Pb^*$ is required (reported as an isotopic ratio in the table), since it is the starting point of the sample Th/U calculation. The study should describe how the initial daughter disequilibrium correction was performed, namely whether a value for Th/U_{liquid} was assumed (with its uncertainty), or whether a constant D_{Th}/D_U partition coefficient ratio (and uncertainty) was used (Rioux et al., 2015; Samperton et al., 2015; Wotzlaw et al., 2014). While secular equilibrium in the melt is usually assumed, this assumption has been demonstrated to be false in some circumstances (Neymark et al., 2000). The magnitude and thus importance of this correction varies according to the sample age and question being asked, so while this information must be reported, it may be appropriate to do so in the methods section, or it may be important to report this directly in the data table (as shown in Tables S1 and S2).

3.3.3. Radiogenic and Sample Isotope Ratios

Whether or not the material has substantial amounts of initial Pb will determine which isotope ratios are reported (Tables S1 and S2), as will the method of common Pb correction, i.e., whether it is subtracted based on an estimate of its composition or whether it is calculated using an isochron approach (see Section 5). For samples with negligible initial Pb_c, such as zircon and baddeleyite, or for those for which the initial Pb_c composition can be reasonably estimated, radiogenic isotope ratios (corrected for mass fractionation, tracer, and analytical blank Pb and U contributions, and any residual initial Pb content) should be reported. In this case, the three radiogenic isotope ratios, $^{206}Pb^*/^{238}U$, $^{207}Pb^*/^{235}U$, and $^{207}Pb^*/^{206}Pb^*$ and their associated relative (percentage) uncertainties are required to compute the covariance structure in ID-TIMS U-Pb measurements; thus, they should always be reported. Reporting the correlation coefficient between $^{206}Pb/^{238}U$ and $^{207}Pb/^{235}U$ is required for calculation and visualization of radioisotope dates and derived geological ages in a concordia plot (see Figs. 2A and 3A). We also recommend that these ratios be reported both with and without correction for initial ^{230}Th disequilibrium, given that this correction requires significant interpretation. While it is acceptable to report either corrected or uncorrected ratios, and the appropriate approach may depend on the particulars of a study, it is important to note that a reader cannot reproduce concordia plots without having corrected ratios. Similarly, in rare cases where ^{231}Pa disequilibrium is considered significant, both corrected and uncorrected ratios should be reported. Usually, it is acceptable to ignore the ^{231}Pa altogether, because other than in some extreme examples (Anczkiewicz et al., 2001), its magnitude is tiny (Schmitt, 2007) and largely speculative.

For samples where the initial Pb correction has a large uncertainty, and/or if the data are to be used for isochron calculations, the sample isotope ratios should be reported (corrected for mass fractionation, ± disequilibrium, and tracer and analytical blank Pb and U contributions, but not initial Pb contents), as shown in Table S2. In this case, reporting the ratios $^{238}U/^{206}Pb$, $^{207}Pb/^{206}Pb$, and $^{204}Pb/^{206}Pb$ and their associated relative (percentage) uncertainties and uncertainty correlations allows the use of two- and three-dimensional Tera-Wasserburg constructions to simultaneously solve for the concordia intercept ($^{206}Pb/^{238}U$) date and initial Pb composition for a set of analyses representing variable mixtures of radiogenic and initial Pb (Ludwig, 1998). We recommend reporting these total sample ratios whenever significant quantities of initial Pb are present in samples. We also recommend that these ratios be reported both with and without correction for initial ^{230}Th disequilibrium. Similarly, in rare cases where ^{231}Pa disequilibrium is thought to be significant, both corrected and uncorrected ratios should be reported. As with high Pb^*/Pb_c minerals, it is acceptable to report either corrected or uncorrected ratios, and the appropriate approach may depend on the particulars of a study, but again it is important to note that a reader cannot reproduce concordia plots, or perform isochron calculations, without having corrected ratios.

Downloaded from http://pubs.geoscienceworld.org/gsa/gsabulletin/article-pdf/136/9-10/4233/6898541/b37321.1.pdf
by guest

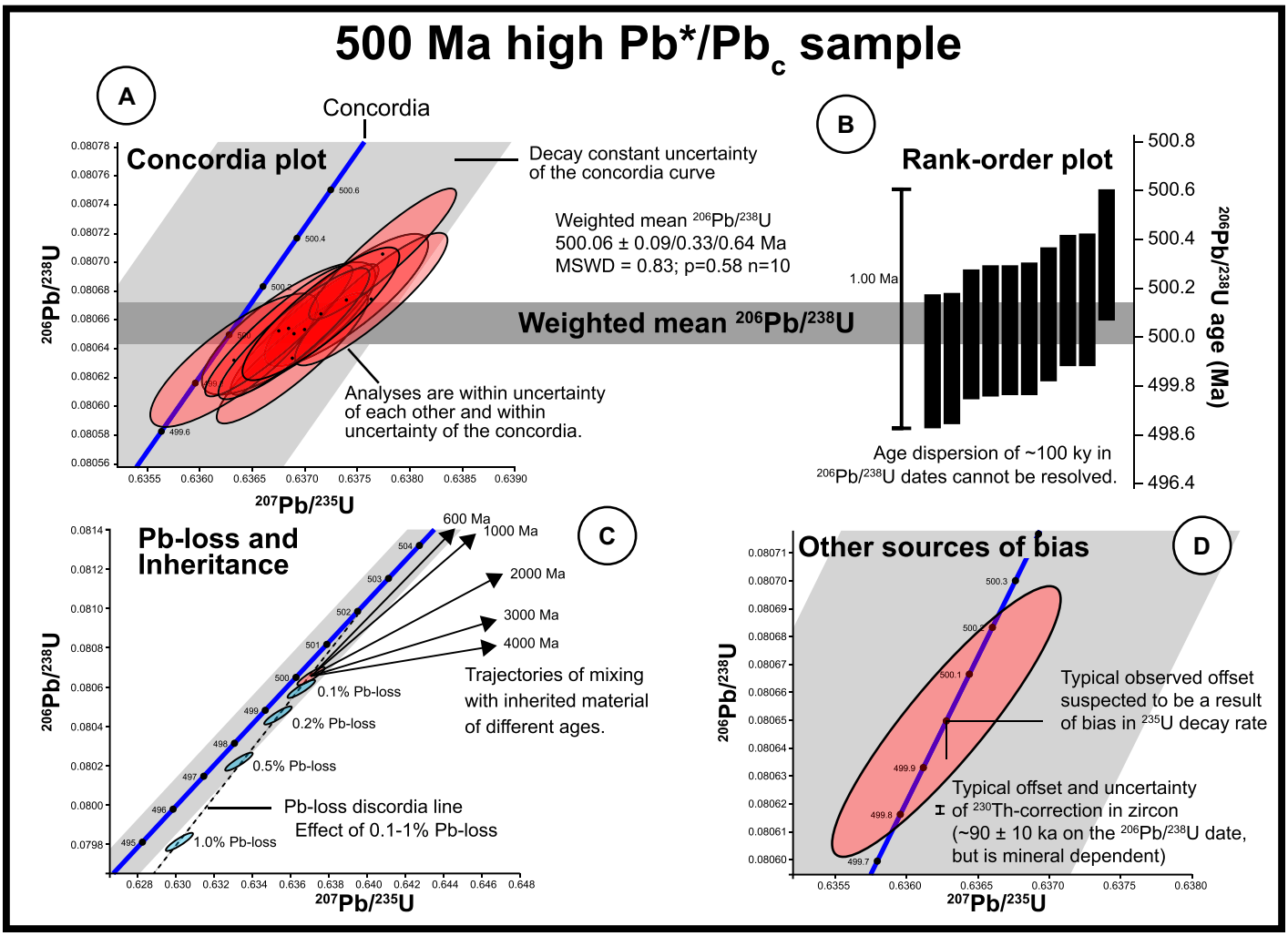


Figure 2. Impact of different types of system complexity on precise U-Pb dates in Wetherill concordia plots and age ranked plots for analyses of a 500 Ma high Pb*/Pb$_c$ sample. (A) Concordia plot of high Pb*/Pb$_c$ analyses situated within concordia curve uncertainty. Excellent reproducibility (mean square of weighted deviates [MSWD] = 0.83) allows for calculation of a weighted mean age. (B) Representation of the ^{206}Pb/^{238}U dates in a rank order plot; individual dates are statistically equivalent and do not resolve a hypothetical 100 k.y. duration of mineral growth. (C) High Pb*/Pb$_c$ analyses delineating a lead-loss trend that becomes visible at >0.5% Pb-loss at the chosen uncertainty of individual dates. Graph also shows different mixing trajectories toward xenocrystic/inherited components diverging from the concordia, leading to discordance as a function of the age of the xenocrystic component as well as of the analytical precision. (D) Effect of ^{230}Th disequilibrium on a 500 Ma zircon with a high Pb*/Pb$_c$ level as well as on suspected λ_{235U} inaccuracy (see text for discussion). Expected shifts in the concordia space stay within the analytical uncertainty ellipse and the decay constant uncertainty band of the concordia, respectively. Amount of ^{230}Th disequilibrium and its uncertainty will be different for different minerals; e.g., see Parrish (1990).

3.4. Date Calculation

For samples where an initial Pb subtraction is conducted (in addition to a blank Pb subtraction), one should report the dates calculated from the radiogenic isotope ratios in the data table, along with their 2-sigma uncertainties (Table S1). These can then be readily used by others for inspection and to produce plots. Three dates can be computed from the ^{206}Pb*/^{238}U, ^{207}Pb*/^{235}U, and ^{207}Pb*/^{206}Pb* isotope ratios and the decay constants of ^{238}U and ^{235}U. The values and propagated uncertainties of the dates calculated from the isotope ratios are required to assess concordance and compute more complex geological age models. We recommend these dates be reported corrected for initial ^{230}Th and ^{231}Pa daughter isotope disequilibrium, though in some cases this correction is significant enough that it is useful to report dates without the disequilibrium correction, or even to report the dates with multiple corrections (perhaps in a separate table and/or with separate discussion) using different interpretations for the Th/U$_{liquid}$ (e.g., Rioux et al., 2012). The decay constants used in the date calculation need to be reported (see Section 5.2.2.). For samples greater than a few hundred million years old, it is also useful to provide a measure of discordance for the reader; this is usually reported as a percent difference between the ^{207}Pb/^{206}Pb and ^{206}Pb/^{238}U dates. Conventionally, discordance is positive when the ^{206}Pb/^{238}U date is younger than the ^{207}Pb/^{206}Pb date. If individual dates are interpreted as ages and discussed in the text as such, they should be reported in the ± X/Y/Z format (see Section 5.2).

For analyses of minerals that contain high initial Pb and low Pb*/Pb$_c$ (such as, e.g., apatite, perovskite, or carbonate), and the initial Pb

Downloaded from http://pubs.geoscienceworld.org/gsa/gsabulletin/article-pdf/136/9-10/4233/6898541/b37321.1.pdf
by guest

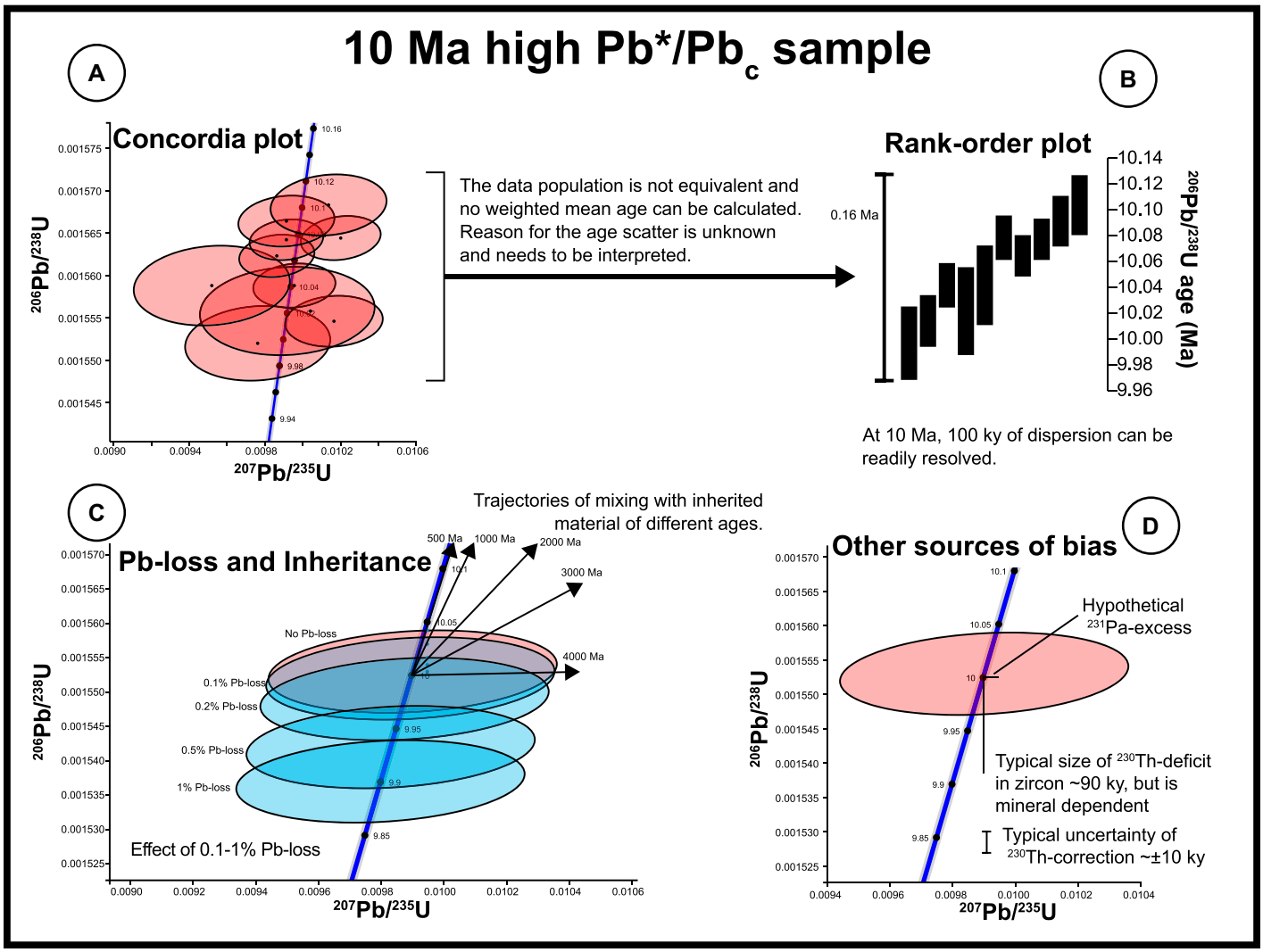


Figure 3. Impact of different types of system complexity on precise U-Pb dates in Wetherill concordia plots and age ranked plots for analyses of a 10 Ma high Pb*/Pb$_c$ sample. (A) Concordia plot of low Pb*/Pb$_c$ analyses from a 10 Ma population showing U decay constant uncertainty band. All individual analyses are intersecting the uncertainty band and are therefore concordant. No weighted mean age can be calculated because the data population is not equivalent; the reason for data scatter is unknown and needs to be explained (see Gaynor et al., 2022a). (B) Rank order plot of the ^{206}Pb/^{238}U dates demonstrates that the 100 k.y. age scatter is readily resolved at an age of 10 Ma. (C) Plot shows 100 k.y. scatter of low Pb*/Pb$_c$ dates that may be interpreted by variable degrees of Pb-loss in individual crystals but cannot be analytically resolved. Example shows that at low Pb*/Pb$_c$ levels, small proportions of xenocrystic/inherited Pb will yield concordant dates and remain undetected (see Gaynor et al., 2022a). (D) Effect of ^{230}Th disequilibrium in a 10 Ma zircon amounts to ~90 k.y. and will lower the ^{206}Pb/^{238}U date outside the analytical uncertainty, while a hypothetical ^{231}Pa excess remains undetected. Amount of ^{230}Th disequilibrium and its uncertainty will be different for different minerals; e.g., see Parrish (1990).

composition is considered a large uncertainty contribution for which numerous interpretations may be valid (e.g., 2-D or 3-D isochron projections are required to arrive at a date; Fig. 4; Table S2; see Sections 5.1.2 and 5.1.5), the data reporting format of Table S2 would apply. In this case, dates may or may not be reported in the data table depending on the Pb*/Pb$_c$ and the authors' interpretation of the data set. If Pb*/Pb$_c$ is somewhat elevated, and the initial Pb isotope composition can be assessed through measurement of a cogenetic U-free mineral phase that has the same initial Pb composition, or there is some other preferred interpretation for the initial Pb isotope composition (such as using an estimate of Pb composition from a whole-earth Pb isotopic evolution model; Stacey and Kramers, 1975), then radiogenic isotope ratios and dates could be reported in the data table (see Table S2). In such a case, the same criteria for ^{230}Th disequilibrium-corrected dates applies here. Alternatively, where an isochron approach is required such that a date is based on a set of individual analyses, the dates or ages may be presented and discussed in the text and relevant figures (or potentially a different table with multiple interpretations of dates). Note that all isochron calculations must be performed on ratios corrected for ^{230}Th disequilibrium.

4. DATA ARCHIVING

Recently, geochronology, like other sciences, is making efforts to improve the infrastructure

Downloaded from http://pubs.geoscienceworld.org/gsa/gsabulletin/article-pdf/136/9-10/4233/6898541/b37321.1.pdf
by guest

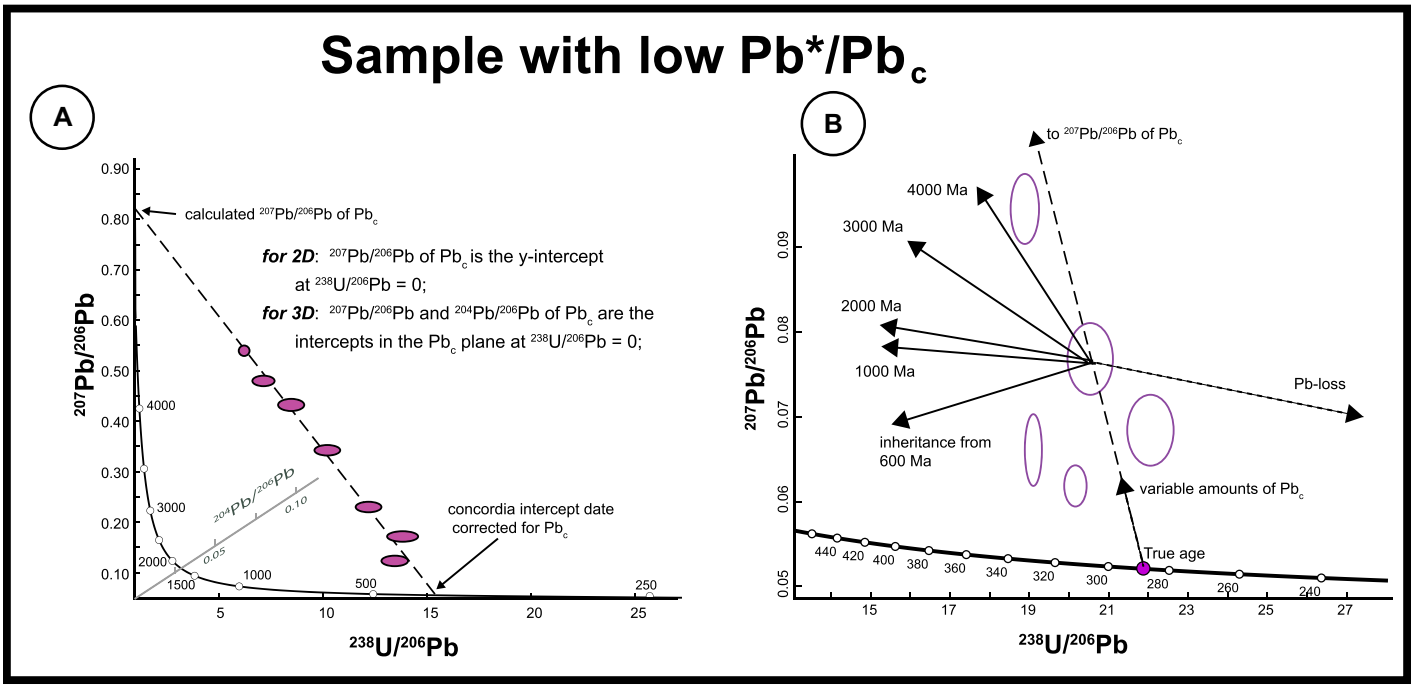


Figure 4. Impact of different types of system complexity on U-Pb dates from minerals with high abundance of common Pb (Pb$_c$) in Tera-Wasserburg Concordia plots. (A) Standard 3-D Tera-Wasserburg diagram illustrating means of calculating an age and the initial ^{207}Pb/^{206}Pb and ^{204}Pb/^{206}Pb isotope compositions of Pb$_c$ for a set of low Pb*/Pb$_c$ analyses. (B) Enlargement of the Pb* intercept area of a standard 3-D Tera-Wasserburg diagram illustrating the effects of various sources of scatter in low Pb*/Pb$_c$ minerals (inherited Pb components of different age, variable amounts of Pb$_c$, and loss of Pb*).

for what has become known as FAIR principles (Findability, Accessibility, Interoperability, and Reusability; Wilkinson et al., 2016) in data management. Recent concerted cyber-infrastructure efforts (e.g., Bowring et al., 2011; McLean et al., 2011; Quinn et al., 2021) have created a way for authors to archive all measured data, data reduction parameters, and results with complete traceability, in a well-described, computer-readable database that allows users to download and reinterpret full data sets. This provides the ultimate data reporting solution and guarantees the utility and longevity of U-Pb data in a way that is publicly available and computer searchable (for instance, by geography, geologic context, or date). Geochron (geochron.org) is a database that will accept and curate data from anyone, and we recommend its use for those publishing geochronological data of all types. Other community accessible databases exist (e.g., Pangea) and will accept generic data types for long-term archiving. A number of geochronology-specific databases exist (e.g., U.S. Geological Survey and AusChem), and while easily accessible and searchable, they may only accept data from certain users.

Despite this progress in achieving FAIR practices, a concise U-Pb data table provided with a publication (as, e.g., Tables S1 and S2) remains instrumental in supplying a reader with an immediate understanding of data alongside the authors' detailed interpretation. Now, it is common to include data tables as supplemental information stored online by the journal, as opposed to printed in the main text of the publication, and we recommend that this trend continue in parallel with more sophisticated data archiving initiatives under the FAIR guidelines. These data should be open source, and reported in a format that is easy for others to open, explore, replot, etc., such as a .csv or Excel file, instead of or in addition to a .pdf.

5. DATA VISUALIZATION AND UNCERTAINTIES

The data and metadata that are recommended above for reporting should be sufficient for exploring and interrogating the data set from many different angles. Part of interpreting these data involves plotting the data for visual inspection, describing interpretations for readers, and inspiring hypothesis testing. Here, we summarize the most popular ways of visualizing ID-TIMS U-Pb data, which can be instrumental in age interpretations (Section 6), and also briefly discuss ways of reporting both random and systematic uncertainties. We only partly reproduce these plots (Figs. 2–4), as this has been done in many other publications (e.g., Corfu, 2013; Reiners et al., 2017; Schaltegger et al., 2015; Schoene, 2014); readers are referred to these resources for more detail. Tools for data visualization and calculations have been developed for geochronology and can be used to make plots. For decades, the community had Isoplot (Ludwig, 1991), which was developed to run in both DOS and Excel, and more recently this general capability has been developed to run in R and/or through an online interface (IsoplotR; Vermeesch, 2018).

5.1. Data Visualization

5.1.1. Wetherill Concordia Plot

U-Pb data have traditionally been plotted on the conventional (Wetherill) concordia plot (^{207}Pb*/^{235}U versus ^{206}Pb*/^{238}U; Wetherill, 1956) for its ability to visualize the concordance of the three radioisotope dates (^{207}Pb*/^{206}Pb*, ^{207}Pb*/^{235}U, and ^{206}Pb*/^{238}U). This conventional form of the concordia plot remains one of the most useful visualizations of concordance of U-Pb data (Figs. 2A and 3A). Accurate plotting of data in the conventional concordia plot requires knowledge of the covariance structure of the isotope ratio uncertainties due to the signifi-

Downloaded from http://pubs.geoscienceworld.org/gsa/gsabulletin/article-pdf/136/9-10/4233/6898541/b37321.1.pdf
by guest

cant correlation of uncertainties of $^{207}Pb^*/^{235}U$ and $^{206}Pb^*/^{238}U$. Uncertainty correlations are equally important for the calculation of "discordia" lines that connect variably discordant data with the concordia curve (see further discussion of "upper intercept ages" below). Although discordance due to Pb-loss becomes less obvious in Phanerozoic samples, discordance due to significantly older xenocrystic inherited cores is readily apparent in this construction (Figs. 2C and 3C). We suggest that the concordia curve always be displayed with its uncertainty stemming from the $\lambda^{238}U$ and $\lambda^{235}U$ uncertainties (see Section 5.2.2), which are visible as an uncertainty band in the concordia plots of Figures 2–4.

5.1.2. Tera-Wasserburg Concordia Plot

The alternative Tera-Wasserburg (T-W) concordia of $^{207}Pb/^{206}Pb$ versus $^{238}U/^{206}Pb$ can be constructed to visualize discordance and calculate discordia lines and intercept ages in ways that are computationally equivalent to the traditional concordia plot (Fig. 4A). The tighter curvature of concordia through the Proterozoic in this construction makes it attractive for visualizing both very ancient and very young samples. However, the primary use of the T-W concordia plot has been for plotting total sample isotope ratios (corrected for fractionation, tracer, and blank contributions, but including the initial common Pb; see Table S2), and it has gained added value for its ability to constrain mixing lines between radiogenic (lower concordia intercept) and initial Pb (y-intercept) end members in samples of variable and low initial U/Pb. This construction is recommended as an alternative visualization for such systems, although its utility is compromised by Pb-loss. As with the conventional concordia diagram, uncertainty correlations must be provided in the data table to plot and perform calculations on the T-W diagram.

5.1.3. Rank Order Plot

Plots of individual U-Pb dates in rank order can provide a useful visualization of the dispersion for many aliquots of a sample or different samples. Rank order plots are particularly useful when only one isotope system is particularly important for the age interpretation, for example, the $^{207}Pb^*/^{206}Pb^*$ date of ancient samples or the $^{206}Pb^*/^{238}U$ date of younger (Phanerozoic) samples (Figs. 2B and 3B). We recommend a combination of concordia and ranked date plots for comprehensive visualization of U-Pb data sets.

5.1.4. Probability Density Function

For data where the range of U-Pb dates is much larger than uncertainties on individual analyses, the probability density function can provide a clear visualization of the distribution of variance across a data set. The probability density function can be used to recover the dominant modes from a set of dates, while the cumulative probability function is the starting point for several algorithms that compare nonparametric distributions (e.g., Kolmogorov–Smirnov test and Kullback-Leibler divergence measure). Probability density functions have been used to visualize the deconvolution of interpreted age populations in mixture modeling (Sambridge and Compston, 1994), and to illustrate comparative age interpretations using different radioisotope chronometers and techniques (Rivera et al., 2014; Schmitz and Kuiper, 2013).

5.1.5. Isochrons

The most widely used isochrons in modern U-Pb geochronology are those calculated in a 2-D or 3-D Tera-Wasserburg concordia diagram (Ludwig, 1998; Wendt, 1984; Zheng, 1992), because they permit both the calculation of the common Pb composition of a sample set and the age of those samples. As with all isochrons, the data must meet the assumptions that all dated materials are the same age, they all have the same common Pb composition, and they all have remained closed systems, which can be evaluated with both geologic context and statistical approaches. Numerous algorithms have been published for both calculating and evaluating linear fits to data with correlated and uncorrelated uncertainties (e.g., McLean et al., 2011; York, 1968; York et al., 2004), and these uncertainties can be propagated in addition to systematic uncertainties such as decay constants to calculate robust concordia intercept dates (Ludwig, 1998). Other types of isochron diagrams (e.g., a traditional $^{238}U/^{204}Pb$ versus $^{206}Pb/^{204}Pb$ isochron, or a $^{204}Pb/^{206}Pb$ versus $^{207}Pb/^{206}Pb$ isochron commonly used in meteoritic studies) can also be plotted and dates calculated using the sample ratios for the high common Pb minerals recommended above.

5.2. Reporting Random and Systematic U-Pb Uncertainties

As the workflow for the data reduction in ID-TIMS U-Pb geochronology is more clearly articulated, it has become clear that it is typically not as simple as reporting a date with a single uncertainty, both within the U-Pb system and also when comparing dates with those of other radioisotopic dating methods (Min et al., 2000; Renne et al., 1998; Schoene et al., 2006). This section details common nomenclature for types of uncertainty in general and specifically for ID-TIMS U-Pb geochronology, and we also review some of the more common sources of systematic uncertainties that were alluded to in Section 3.

5.2.1. Reporting Random and Systematic Uncertainties

During the past two decades there has been a marked increase in analytical precision concurrent with increased intercomparison of ID-TIMS U-Pb data among laboratories, at or close to the quoted level of precision (Kennedy et al., 2014; Nasdala et al., 2018; Schaltegger et al., 2021; Sláma et al., 2008). Also important is being able to compare U-Pb data with data sets from other radioisotopic dating methods despite the systematic uncertainties and biases of the methods (Gradstein et al., 2020; Min et al., 2000; Renne et al., 1998; Sageman et al., 2014). A response to this situation has been to report U-Pb age uncertainties at several different levels of inclusion of systematic uncertainties (Schoene et al., 2006). The first level of age uncertainty (X) reflects the analytical (sometimes called internal) uncertainty associated with determining the U/Pb ratio for a given sample, such that dates from within the same data set can be compared at the highest level of precision. The second level of uncertainty (Y) is the X uncertainty combined with the uncertainty of the tracer calibration. The third level (Z) combines the Y uncertainty with the decay constant uncertainty (see Section 5.2.2), to facilitate comparison of U-Pb dates with other decay systems (this is sometimes called full systematic uncertainties). As a result, it is common and recommended to report ages as Age ± X/Y/Z (always with 2-sigma uncertainties; Figs. 2A and 2B). We recognize that it may be cumbersome to report dates in this way everywhere in a manuscript, especially if only X uncertainties are required for the interpretation, so we recommend that the full ± X/Y/Z be reported somewhere in the publication such that others can compare other data sets at the appropriate level of precision. This is typically reported for an age with an interpreted geologic significance, and not for every date (see Section 6). This facilitates comparison of U-Pb ages determined at different labs with different protocols and also comparison with ages determined by other methods (astrochronology, $^{40}Ar/^{39}Ar$, Rb-Sr, etc.).

5.2.2. Half-Lives and Their Associated Uncertainties

The decay constants $\lambda^{238}U$ and $\lambda^{235}U$ have both been determined by counting experiments (Jaffey et al., 1971) to be ±0.11% and ±0.14%, respectively, and the uncertainties can be plotted with the concordia curve for visualization purposes (Figs. 2 and 3). Following the primary experimental data of Jaffey et al. (1971), Mattinson (2000) demonstrated how U-Pb analyses of closed system zircon using gravimetrically calibrated tracers could allow for determina-

Downloaded from http://pubs.geoscienceworld.org/gsa/gsabulletin/article-pdf/136/9-10/4233/6898541/b37321.1.pdf
by guest

tion of $\lambda^{238}U/\lambda^{235}U$ with higher precision than the existing counting data. Two studies (Mattinson, 2010; Schoene et al., 2006) have presented demonstrably closed system U-Pb zircon data sets to determine $\lambda^{238}U/\lambda^{235}U$ and infer a more accurate value for $\lambda^{235}U$ relative to $\lambda^{238}U$. Those studies show that use of the Jaffey et al. (1971) decay constants may result in analytical points shifted off concordia toward slightly too high $^{207}Pb/^{235}U$ ratios, but within the decay constant uncertainties of Jaffey et al. (1971; Figs. 2A and 2D). New determinations of $\lambda^{238}U$ and $\lambda^{235}U$ are underway (Parsons-Davis et al., 2018) and, depending on the outcome of these experiments, it is possible that the U-Pb community will shift to using a new set of values/uncertainties for $\lambda^{238}U$ and $\lambda^{235}U$. As such, it is important that studies report what decay constant values are used, because some studies (e.g., the Geologic Time Scale 2020; Gradstein et al., 2020) have adopted the empirically revised $\lambda^{235}U$ relative to $\lambda^{238}U$, whereas most have not.

5.2.3. Uranium Isotope Composition

A value of $^{238}U/^{235}U = 137.88$ was used for over 40 years for U-Pb geochronological studies (Steiger and Jager, 1977) based upon a compilation of data from uranium ore bodies (Cowan and Adler, 1976), and was considered invariable. More recently, studies have documented natural variability in $^{238}U/^{235}U$ (Hiess et al., 2012; Stirling et al., 2007; Weyer et al., 2008). Based on a study of $^{238}U/^{235}U$ determinations on U-bearing minerals, we suggest that the value of 137.818 ± 0.045 (2-sigma; Hiess et al., 2012) is representative for zircon U-Pb geochronology. This data set has been augmented by a similar $^{238}U/^{235}U_{zircon}$ study (Livermore et al., 2018) on large zircon aliquots, and another on single grains of zircon (Tissot et al., 2019), both of which show that using the value of Hiess et al. (2012) with its uncertainty is an adequate approach for labs using a ^{233}U-^{235}U tracer, but that it may be possible and definitely preferable to measure the $^{238}U/^{235}U_{zircon}$ for individual dated zircons routinely in the future using a ^{233}U-^{236}U-Pb tracer. The initial data set from Hiess et al. (2012) also shows some indication of variability in minerals other than zircon (e.g., monazite and titanite; see also Ling et al., 2017), and this should be explored further.

5.2.4. Repeatability and Reproducibility

The accuracy of U-Pb dates produced by ID-TIMS should be assessed by reporting standard data acquired under similar conditions and rigor as those of the sample data sets. Examples of standard data reported include natural zircon standards described in the literature (Black et al., 2003; Eddy et al., 2019; Kennedy et al., 2014; Santos et al., 2017; Wall et al., 2016; Wiedenbeck et al., 1995), and synthetic standards that have been mixed and distributed to labs (Condon et al., 2008; Schaltegger et al., 2021; Schoene et al., 2015). To be used as natural reference materials, they are ideally of identical composition (matrix-matched), have been analyzed in multiple U-Pb ID-TIMS laboratories, and the U-Pb community has reached consensus on their isotopic composition and age. There has been much effort to calibrate natural zircon reference materials, and similar efforts are required for other U-bearing minerals. These efforts are partially motivated by the need of the in situ dating community for natural standard material.

The advantage of synthetic reference solutions is that they are inherently homogeneous, whereas natural mineral standards are frequently demonstrated not to be. The downside of synthetic reference solutions is that they may not be treated in the same way as unknowns; for example, they may not be put through ion separation chemistry as the unknowns are. However, it is possible to put synthetic solutions through the entire procedure (except for chemical abrasion) just like mineral unknowns, and this is recommended for testing comparability.

While it is ideal to report new standard data with each study for standards analyzed during the same time period as the unknowns, it can be acceptable to refer to a report of the respective laboratory that can be accessed via a DOI link (though there is no currently accepted protocol for doing this in geochronology), or perhaps even a complementary publication with standard data included. If opting for the latter, then the standard data should have been collected in the same lab, using the same methods, and analyzed over the same period of time. Ultimately, if the materials are themselves homogenous, a study can assess excess scatter in sample dates relative to standard data produced over the same time period, to facilitate comparison of data sets among laboratories if they each report standard data from the same material.

5.2.5. Other Sources of Systematic and Random Uncertainty

Understanding whether each source of uncertainty is random/internal or systematic/external is important. This impacts how data, dates, and ages are interpreted and compared. For example, if one were to propagate the systematic decay constant uncertainty into each data point of a set of $^{206}Pb/^{238}U$ dates, and then take a weighted mean of those dates, the addition of the decay constant uncertainty would reduce potentially real dispersion in dates, and also the systematic uncertainty would be incorrectly minimized in the weighted mean. Hence, systematic uncertainties must be incorporated into statistically derived dates (e.g., weighted mean or isochron dates) by propagating them onto weighted mean uncertainties. This can be done by calculating a weighted mean date of a set of isotopic ratios such as the $^{206}Pb^*/^{238}U$ and then using standard uncertainty propagation for the decay constant during the age calculation. Some software packages will do this automatically (McLean et al., 2011).

Some sources of uncertainty do not fit so easily into the categories of random and systematic so that their propagation is not as straightforward. For example, these include (1) the assumed Th/U value of a melt or liquid from which a mineral crystallized, which is used to make the ^{230}Th disequilibrium correction; (2) the correction for instrumental mass fractionation of samples that are not double spiked; and (3) the subtraction of spike and Pb_c isotopes from the sample. As an example, the Th/U of each zircon may be slightly different such that the disequilibrium correction and its uncertainty are not entirely systematic (Figs. 2D and 3D). However, the amount and uncertainty of this correction end up being very similar for each analysis, so that the uncertainty on a weighted mean date of many analyses would act to inaccurately minimize the uncertainty in the disequilibrium correction (Crowley et al., 2007; Ickert et al., 2015). Understanding the nature of the sources of uncertainty and how they affect the age uncertainty is critical, and algorithms developed to accurately propagate uncertainties that fit into this category (McLean et al., 2011) should be used when applying statistical models to data sets.

Lastly, while it is common to propagate uncertainties associated with standard reproducibility into unknowns in some fields, especially those based on sample-standard bracketing to correct isotopic and elemental ratios for unknowns (e.g., Horstwood et al., 2016), this potentially systematic source of uncertainty is not typically reported in ID-TIMS U-Pb geochronology. Going forward, we recommend that relevant standard data be published with unknowns to assess reproducibility, and when appropriate, this uncertainty be considered when interpreting dispersion in unknowns (dates).

6. GEOLOGICAL AGE INTERPRETATIONS: FROM DATES TO AGES

One of the greatest challenges in geochronology is deriving a geologically meaningful "age" from a collection of isotope ratio data and derived dates. Recall that parent/daughter isotope ratios are converted into "dates" using the decay equation and appropriate decay constants.

Downloaded from http://pubs.geoscienceworld.org/gsa/gsabulletin/article-pdf/136/9-10/4233/6898541/b37321.1.pdf
by guest

Dates or isotope ratios (in the case of isochrons) are then subjected to qualitative and quantitative analysis and interpreted in terms of a geologic age. This process has changed over time as analytical precision, sampling technique, and associated analytical tools have improved.

As ID-TIMS U-Pb geochronology has become more precise, dates of zircon, baddeleyite, or monazite, for example, commonly show dispersion beyond analytical uncertainty. Initially, with uncertainties at the several permil level and multi-grain fractions being analyzed, and limited tools for dealing with Pb-loss, dispersion was thought to result from both Pb-loss and the incorporation of older inherited material (see reviews in Corfu, 2013; Schaltegger et al., 2015; Schoene, 2014). Precision has increased by nearly an order of magnitude to modern levels, along with a similar reduction in sample size. Modern approaches use chemical abrasion on single minerals and fragments, such that dispersion in data sets can be more confidently argued to be due to geologic processes (Figs. 2C and 3C). Examples of an ~10 m.y. old mineral population with such excess scatter in $^{206}Pb/^{238}U$ dates are shown in Figures 3A and 5C. Therefore, attaching significance to a date requires an interpretation as well as an understanding of mineral saturation, crystallization, dissolution, and element mobility in igneous and metamorphic systems, in addition to the analytical considerations outlined above.

Even a single phase of crystallization will be finite and can be protracted over measurable time scales (Rivera et al., 2013; Samperton et al., 2017; Wotzlaw et al., 2013), and so ID-TIMS U-Pb geochronology is not only faced with these complications, but is also driving the science behind understanding them. This acknowledgment of protracted or multiphase crystallization histories has become increasingly important because (1) we have a better ability to quantify (in the case of thermochronology) or minimize (in the case of chemical abrasion of zircon) Pb-loss; (2) a growing database of experimental and geological case studies from different environments provides a theoretical framework for explaining dispersion in U-Pb dates; and (3) imaging and microanalytical tools are increasingly available and useful for testing hypotheses for the cause of date dispersion (Beckman et al., 2014; Bowring et al., 1989; Compston et al., 1984; DesOrmeau et al., 2018; Keller et al., 2019; Kelly and Harley, 2005; Kohn, 2016). Although the addition of textural, petrologic, and geochemical information to chronological data is not new, it continues to become more sophisticated and necessary as part of an emerging field called "petrochronology" (e.g., Kohn et al., 2017). Reviewing all of this material is beyond the scope of this paper, but it is important to illustrate that data interpretation in context is a critical part of determining and publishing ages, and that authors should acknowledge this point. Below, we review the variety of tools available, from analytical to statistical, and encourage workers to discuss the benefits and drawbacks transparently in publications.

6.1. Recognizing and Resolving Pb-loss

Recognizable open system behavior (i.e., discordance) is commonly attributed to loss of Pb, which has been a limitation in U-Pb geochronology since its invention (Corfu, 2013). The chemical abrasion technique (or CA-TIMS; Mattinson, 2005) is the most effective way of reducing or eliminating the effects of Pb-loss in zircon. This procedure removes zones of higher uranium concentration, and therefore zones of higher degrees of decay-induced crystal damage that would have facilitated Pb-loss. The partial dissolution step of chemical abrasion selectively removes such zones at the micron scale (Burgess et al., 2014; Davydov et al., 2010; Huyskens et al., 2016; Mattinson, 2010; Mattinson, 2011; McKanna et al., 2023; McKanna et al., 2024; Mundil et al., 2004; Widmann et al., 2019) and leaves behind a residue of zircon with lower U content that has a greater probability of having remained a closed chemical system through time. This empirical procedure is preceded by a thermal annealing step that should re-equilibrate radiation-damaged domains. Chemical abrasion should nearly always be used in ID-TIMS U-Pb zircon geochronology, though it should be kept in mind that this procedure is imperfect, and there are plenty of examples where individual zircon grains have been interpreted to carry residual Pb-loss following chemical abrasion (e.g., Davydov et al., 2010; Gaynor et al., 2022b; Mackinder et al., 2019; Ovtcharova et al., 2015; Ramezani et al., 2007; Schoene et al., 2010a; Zhou et al., 2019). Whereas Pb-loss may be readily recognizable in high Pb^*/Pb_c data sets (Fig. 2C), especially in minerals older than ca. 1 Ga (Mungall et al., 2016; Scoates and Friedman, 2008), it may be undetectable at low Pb^*/Pb_c levels due to large uncertainties resulting from the Pb_c correction, and in rocks less than ca. 300 Ma, where Pb-loss trajectories parallel the concordia curve (Fig. 3C). While metamict zircon has been shown, in some cases, to be geochemically distinct from pristine zircon (Bell et al., 2019; Keller et al., 2019), thus far this has not been a consistent indicator of Pb-loss (McKanna et al., 2024). Clearly, even more detailed studies are required to better understand the mechanics of the CA-TIMS procedure, how to best enhance and evaluate its efficacy on a case-by-case basis, and how to assess whether it results in an age bias (e.g., if high-U rims are dissolved). In the meantime, most workers assume chemical abrasion has removed Pb-loss unless there are obvious young outliers in zircon data sets, but it is never known for certain. While chemical abrasion techniques have been explored for other minerals (Peterman et al., 2012; Rioux et al., 2010), there are currently no similarly effective tools for remediating Pb-loss in minerals other than zircon.

6.2. Analytical Tools for Understanding Age Dispersion

Determining the cause of age dispersion in a set of dates from a sample can be aided by using geologic observations in addition to complementary analytical tools to better understand a dated mineral's geologic, textural, petrographic, and geochemical characteristics. For example, relative age constraints, such as stratigraphic superposition or crosscutting relationships, can aid in interpreting complicated geochronological data sets. Imaging by optical microscopy or qualitative evaluation of minerals by scanning electron microscopy, cathodoluminescence, and backscattered electron techniques either in thin section or grain mount can reveal the presence of cores and rims (Figs. 2C and 3C) and other complex internal growth structures (e.g., Corfu et al., 2003), as well as qualitatively assess the extent of metamictization. In situ microbeam analyses can help to identify and avoid inherited components in zircon or other crystals prior to ID U-Pb geochronology by revealing geochemical domains (e.g., Rivera et al., 2013). Further information about crystal composition and growth history can be inferred from Ti-in-zircon or Zr-in-titanite thermometry (Hayden et al., 2008; Watson et al., 2006) and/or trace element contents as indices of magma differentiation (Claiborne et al., 2010; Reid et al., 2011; Samperton et al., 2015). In addition, for ID-TIMS U-Pb geochronology, minerals are dissolved and U and Pb are isolated from other elements using ion exchange chemistry. Now it is becoming more common to measure the chemical (e.g., rare earth element) or isotopic (e.g., Hf, Sr, and Nd) composition of other elements in the sample by ICP-MS to add another layer of information to help with U-Pb date interpretation (Amelin et al., 1999; O'Connor et al., 2022; Schaltegger et al., 2002; Schoene et al., 2010b). Each of these tools can be used to both formulate and evaluate hypotheses regarding progressive growth of dated minerals and can even be used to argue in favor of protracted crystal growth or Pb-loss as the viable mechanism for creating age dispersion in a sample (Schoene and Baxter, 2017; Schoene

Downloaded from http://pubs.geoscienceworld.org/gsa/gsabulletin/article-pdf/136/9-10/4233/6898541/b37321.1.pdf
by guest

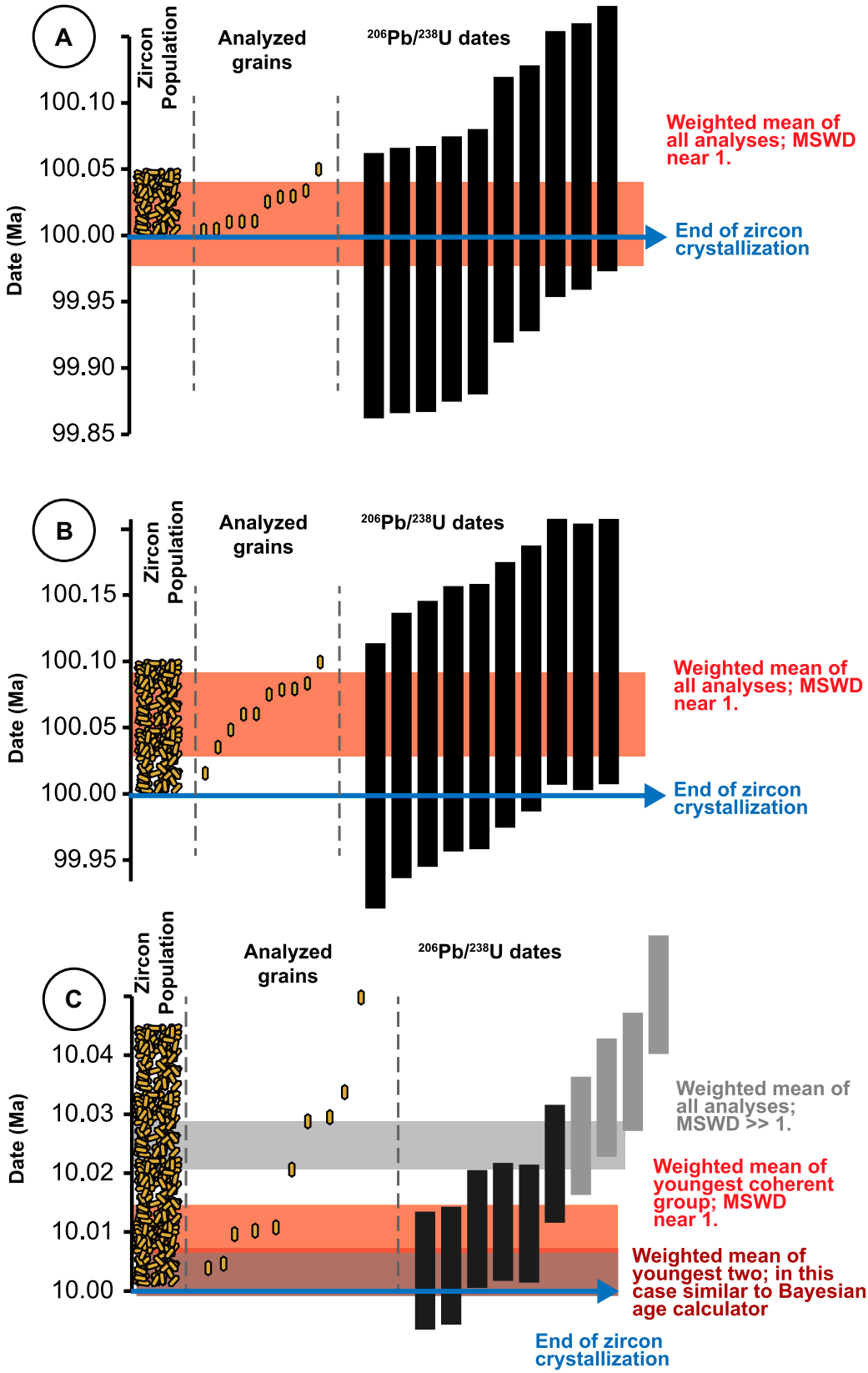


Figure 5. Examples of the relationship between a zircon population, most applicable to igneous rocks, with a subsample of 10 analyzed zircon grains from this population, and the distribution of measured U-Pb dates as commonly plotted in U-Pb geochronology. Magmatic zircon population crystallized over 50–100 k.y., and the zircon grains dated have the same relative age distribution. Analytical uncertainties are 0.1%. Note that each analyzed grain and its corresponding date represents the average age of the whole crystal. In this cartoon, particular grains capture the onset and termination of zircon crystallization, though in reality this may or may not be accurate (see accompanying text). (A) In the case of a 100 Ma igneous rock that crystallized over 50 k.y., featuring magmatic zircon only, the larger absolute uncertainties on the measurements mean that all of the measurements are equivalent (mean square of weighted deviates [MSWD] is ~1). In this case, the weighted mean of all analyses captures the end (but not the beginning) of zircon crystallization. In a volcanic rock, this would accurately date the eruption. (B) Panel depicts the case of a 100 Ma igneous rock that crystallized over 100 k.y. In this case, individual analytical uncertainties largely overlap with the onset and termination of crystallization, but a weighted mean records neither, despite having a MSWD of ~1. Inaccuracy of this weighted mean date may remain undetected. (C) In the case of a 10 Ma igneous rock featuring magmatic zircon only, the 50 k.y. age spread is clearly resolved with uncertainties of ± 10 k.y. Weighted mean of the entire data set yields a high MSWD value and would not likely be interpreted as a geologic event. Weighted mean of the youngest coherent group (here, the youngest six measurements, with a MSWD of ~1) yields a nominally precise value but does not correspond to any geological event, such as, e.g., the end of zircon crystallization or volcanic eruption. Alternative interpretations of this data set include a weighted mean of the youngest two, just using the youngest date, or applying a Bayesian model to the entire range of analyses to determine a probabilistic estimate of the cessation of zircon crystallization.

Downloaded from http://pubs.geoscienceworld.org/gsa/gsabulletin/article-pdf/136/9-10/4233/6898541/b37321.1.pdf
by guest

et al., 2015; Szymanowski et al., 2017; Wotzlaw et al., 2013). While not all studies require this level of detail, we recommend using these analytical tools when necessary to marshal the most objective interpretation of U-Pb dates into geologically meaningful ages.

As analytical blanks decrease and the sensitivity of mass spectrometers increases, dating of increasingly small domains of minerals has become possible, whereby it is no longer uncommon to fracture and analyze fragments of individual grains to explore age heterogeneity within single grains, which can be used to investigate dispersion within a larger sample (Gordon et al., 2010; Hawkins and Bowring, 1997; Samperton et al., 2015; Steiger et al., 1993; Tapster et al., 2016; White et al., 2020). Though there are practical limitations such as analytical imprecision due to reduced Pb* and U in sub-grain samples, we recommend the practice of dating individual crystal fragments to understand intra-grain variation and minimize averaging domains of varying geological age. This will result in a better characterization of the true spectrum of zircon crystallization in a sample (Keller et al., 2018; Klein and Eddy, 2023).

6.3. Statistical Approaches to Age Calculation

As discussed above, it is ubiquitous in U-Pb geochronology (ID-TIMS and otherwise) to use statistical treatments to adequately propagate analytical and systematic uncertainties into models for individual U-Pb dates. It is also common to convolve multiple U-Pb dates into a statistical model that is interpreted to reflect a geologic process—in other words, to assign an age to a set of dates. The most commonly used models are the weighted mean date and isochron date. Isochrons assume that the materials have the same initial isotopic composition, became a closed system at the same instant in time, and have remained a closed system since that moment. The latter two assumptions apply to weighted mean dates as well. These assumptions can always be evaluated but never completely validated. As an essential first pass, it is important to establish whether these assumptions are met based on geological, petrologic, and/or geochemical means. In addition, associated with statistical models like weighted means and isochrons are measures of the goodness of fit, such as the mean square of weighted deviates (MSWD, also known as the reduced chi-squared statistic; Wendt and Carl, 1991; York, 1968) and the related probability of fit. Notably, these measures are related to the precision of the single data points relative to their scatter. If the scatter in the single data points can be predicted by their estimated uncertainty, then the MSWD will be near 1 (Figs. 5A and 5B). Conversely, if the uncertainties of the same data are much smaller than the observed intra-sample variation, then the MSWD or other measure will highlight the lack of coherence (Figs. 3B and 5C). Several recent resources discuss the application of the MSWD in geochronology, and the reader is referred there for more detail (Glazner and Sadler, 2016; Keller et al., 2018; Klein and Eddy, 2023; Reiners et al., 2017). When statistical models are used to calculate dates or assess closed system behavior, it is extremely important that a goodness of fit be reported, because this helps a reader (and an author) to evaluate the accuracy of the age interpretation. However, it is also important to realize that a MSWD near one only indicates that there is no resolvable scatter in the data set, not that the model assumption—that the minerals are in fact the same age—is true (Figs. 5A and 5B). Below, we briefly review the commonly applied models for calculating ages from data sets with variable scatter and magnitude of analytical uncertainty.

6.3.1. Determining an Age from Data Sets with Crystallization Date Variability Smaller than Analytical Uncertainty

In such a case, by no means can we assume that the oldest and youngest dates of the statistically equivalent population represent a duration, though a maximum duration of crystallization can be calculated from such data sets (Glazner and Sadler, 2016; Keller et al., 2018; Klein and Eddy, 2023). It is more common in such cases to use a statistical model such as a weighted mean that treats mineral crystallization as an instant event in time. The accuracy of this assumption can partially be evaluated by whether the MSWD value deviates acceptably from unity (Wendt and Carl, 1991). However, minerals undoubtedly do not crystallize instantly, and in the case of zircon, minerals have been shown to crystallize over many hundreds of thousands of years in some cases (Samperton et al., 2015; Schmitt et al., 2011), which may not be resolvable in some data sets where uncertainties on individual zircons are on the order of hundreds of thousands of years. If analytical uncertainty is too large to recognize the true zircon growth timespan in a sample, a weighted mean date may yield a valid MSWD and a value that is simply the average crystallization time of zircons in that sample, and not necessarily the geologic process targeted (Fig. 5B). On the other hand, some zircon data sets from volcanic rocks have age dispersion of tens of thousands of years or less with comparable analytical uncertainties, which implies that similarly short durations of zircon crystallization may be present even when unresolvable analytically, such that a weighted mean resulting in precision of tens of thousands of years would be accurate. There is currently no reliable way to tell the difference. Therefore, while weighted mean dates increase the precision of an interpreted age as N increases (N being the number of analyses), verifying the assumptions that validate their use remains difficult. As such, weighted mean dates, or isochrons, in which the derived uncertainty is much less than the single data point uncertainty should be treated with caution.

6.3.2. Determining Ages from Complex Populations of Dates

The statistical models described above assume that all data points are representative of the same moment in time. Commonly, however, the dispersion in the distribution of U-Pb zircon dates is greater than the analytical uncertainties (Figs. 3A, 3B, and 5C). Causes may be geological (growth, or a combination of different age components in the same grain; see Gaynor et al., 2022a; Samperton et al., 2015), systemic (Pb-loss through decay damage, variable Th/U of melt, and/or zircon through fractional crystallization), or computational (variation of Pb*/Pb_c amongst analyses, introducing variation of the $^{206}Pb/^{238}U$ date). Below, we briefly mention commonly used approaches for assigning ages to data sets argued to be scattered as a result of geological processes.

In the least constrained case of a continuous distribution of ages with no obvious mode, one can treat each analysis as individually representing the best estimate of the average time of crystallization of that mineral or mineral fragment. This may be useful if there is independent evidence that a spectrum of dates represents continual crystallization and that this continuum records a process of interest, e.g., the cooling of a magma after zircon saturation or the duration of a metamorphic event. In such a case, the oldest date may be used to inform the age of the oldest mineral as the best estimate of the onset of mineral crystallization. Conversely, the youngest date can be used to infer the age of the youngest mineral sampled and to estimate the termination of growth, whether that be a magma's solidus or the "end" of metamorphic growth (Samperton et al., 2017; Schaltegger and Davies, 2017; Taylor et al., 2016). However, it is important to recognize with ID-TIMS U-Pb geochronology, and even to a lesser extent with microbeam techniques, that the date obtained is an average over the measured volume such that it can be difficult to capture the youngest or oldest ages. This can be quantified and modeled to some extent, and such attempts show that the duration of true mineral crystallization will be longer than the measurement indicates, by an

Downloaded from http://pubs.geoscienceworld.org/gsa/gsabulletin/article-pdf/136/9-10/4233/6898541/b37321.1.pdf
by guest

amount of time that depends on factors such as mineral growth rate, nucleation rate, and grain armoring (Curry et al., 2021; Klein and Eddy, 2023). Subtle xenocrystic cores within dated minerals can also skew data sets toward older dates such that the average has no geologic significance (Gaynor et al., 2023). Similarly, subtle Pb-loss may skew the interpretation of the youngest dates. A number of studies present modeling approaches for understanding zircon growth in magmas and attaching significance to a spectrum of dates (Curry et al., 2021; Klein and Eddy, 2023; Ratschbacher et al., 2018; Schaen et al., 2021), and the appropriate approach will depend on the question being asked and the particulars of a data set and study.

Considerations of mineral chemistry, morphology/zoning patterns, or isotopic (e.g., O, Hf) composition can aid in understanding mineral age dispersion and be used to model the process of interest (Chelle-Michou et al., 2014; Eddy et al., 2020; Pamukçu et al., 2022; Rivera et al., 2014; Schoene et al., 2012; Wotzlaw et al., 2013). For example, if a subset of analyses whose dates overlap within uncertainties also have an identical Hf isotopic composition that is different from other analyses in the population, it bolsters an interpretation that they are, in fact, cogenetic, having crystallized rapidly. Similar logic can be applied to either geochemistry or Ti-in-zircon temperatures for a subset of analyses from a population. For example, if a population of zircon dates shows a decrease in age with temperature, this can be used to infer crystallization during cooling (Rivera et al., 2014; Samperton et al., 2017). A similar set of criteria may be applied to other datable minerals but has been less explored in ID-TIMS U-Pb geochronology.

A common process that is interpreted from complicated suites of zircon dates is that of an eruption age for a tuff. In this case, unlike plutonic or metamorphic rocks, it is reasonable to assume that there is a cut-off point at which phenocrysts cease to grow (eruption). While there is consensus that when determining an eruption age, one should focus on the youngest dates from a spectrum, there are multiple approaches to doing this. Selecting the youngest date alone may be the best estimate of eruption of a tuff (Griffis et al., 2018; Kasbohm and Schoene, 2018; Schoene et al., 2010a), as it will be less biased by prolonged growth, but comes at the expense of decreased precision. In addition, this interpretation can also be biased given the possibility the youngest analysis lies at the margins of expected analytical scatter, which increases the possibility that it is too young and/or reflects a minor amount of Pb-loss. Possibly, even younger—but not yet sampled—zircons exist in the population, making the youngest measured date too old. Another popular approach is to calculate a weighted mean age from the youngest analyses that satisfy the acceptable limits of MSWD value (Augland et al., 2019; Eberth and Kamo, 2020; Ramezani et al., 2022; Sahy et al., 2017; Fig. 3A); the same caveats discussed in Section 6.3.1. apply in this case. As an alternative, Keller et al. (2018) ran a series of models that explore the best approach to determining an eruption age from synthetic data sets that vary in terms of the duration of true crystallization versus the analytical uncertainty of individual analyses. Except for cases where the actual crystallization duration is very small relative to the analytical uncertainties, the general conclusion is that weighted means of any number of analyses risk producing overly precise dates that are inaccurate. Keller et al. (2018) instead proposed a Bayesian approach to estimating eruption ages that considers the distribution of dates obtained against an anticipated distribution (prior) to obtain an estimate of eruption and its uncertainty. This model, as with any age interpretation, becomes better at high N and also is better when the assumed, prior distribution of dates matches closely with the sample data set. This and other attempts to ask what N is necessary to characterize a sample population note a great increase in knowledge gained between 10 and 20 data points, and a tapering off at $N > 20$ (Keller et al., 2018; Klein and Eddy, 2023). Therefore, we recommend that when zircon supply is sufficient, 10–20 analyses should be the minimum to yield a robust eruption estimate, regardless of the interpretation approach used.

From the above discussion, we can conclude that: (1) while there has been much progress in understanding how to interpret dispersed U-Pb data sets, no single interpretative framework is entirely correct, and any age interpretation is dependent upon a set of assumptions of varying legitimacy, and evaluating the differences between ages using different interpretative frameworks can be insightful; (2) larger high-precision data sets ($N > 15$–20) afford more leverage for both analytical and statistical discrimination; and (3) additional a priori information (e.g., sample context and mineral chemistry) can lead to more objective interpretations. As such, assigning an age of a geological process to a set of data points becomes an exercise in exploring possibilities, and multiple interpretations are always possible (and indeed are ideally explored and reported in a publication). Importantly, if the recommended data reporting criteria are upheld, then data that appear in publications can be reinterpreted as new approaches and information emerge.

7. CONCLUDING REMARKS

In this paper, we have attempted to provide a summary of the key elements that are combined to derive high-precision ID-TIMS U-Pb geochronology. Some of these issues are specific to isotope dilution U-Pb geochronology (e.g., data reduction); however, many are generic (e.g., dates to ages), and the same principles are applicable to other methods (e.g., LA-ICP-MS U-Pb) and radioisotopic systems (e.g., $^{40}Ar/^{39}Ar$).

Major conclusions that arise from the above are:

(1) All peer-reviewed publications containing geochronological data should, at a minimum, present enough information so that others can reproduce the dates calculated for the samples studied, thus allowing future deconvolution and recalculation. This includes a range of metadata such as basic sample information, sample composition, methods, and laboratory performance. This manuscript attempts to outline what those criteria are.

(2) The geochronologist as a "producer" as well as a "consumer" of geochronological data must be aware of the fact that an "age" is always an interpretative model of radioisotopic results, or "dates." These results and their interpretation(s) should be rigorously separated, and an outline of the hypotheses that were used for age interpretation should be described in detail.

(3) Multiple age interpretations are often possible, and exploring each of these provides an additional way to consider the preferred/reported age uncertainty. Where possible, other types of information should be included to support preferred interpretations.

(4) As the precision of dates and ages continues to increase, the production and publication of standard data comparable on many levels to sample data is becoming increasingly important as a means of assessing intralaboratory and interlaboratory repeatability, and identifying biases.

As with many other Earth science disciplines, geochronology is on the cusp of a digital revolution. Utilizing a rapidly developing cyberinfrastructure that captures the aforementioned data and metadata will increase the longevity of radioisotopic ages and their usefulness (Deering et al., 2016; Paul et al., 2021; Piccoli et al., 2023).

ACKNOWLEDGMENTS

This contribution builds upon decades of development of the ID-TIMS U-Pb system by pioneers in isotope geochemistry and radioisotope geochronology to whom we are indebted. This paper is an outgrowth of the EARTHTIME Initiative and benefited from discussions at several National Science Foundation– and European Science Foundation–sponsored workshops.

Downloaded from http://pubs.geoscienceworld.org/gsa/gsabulletin/article-pdf/136/9-10/4233/6898541/b37321.1.pdf
by guest

REFERENCES CITED

Amelin, Y., Lee, D.-C., Halliday, A.N., and Pidgeon, R.T., 1999, Nature of the Earth's earliest crust from hafnium isotopes in single detrital zircons: Nature, v. 399, no. 6733, p. 252–255, https://doi.org/10.1038/20426.

Anczkiewicz, R., Oberli, F., Burg, J.P., Villa, I.M., Gunther, D., and Meier, M., 2001, Timing of normal faulting along the Indus suture in Pakistan Himalaya and a case of major $^{231}Pa/^{235}U$ initial disequilibrium in zircon: Earth and Planetary Science Letters, v. 191, p. 101–114, https://doi.org/10.1016/S0012-821X(01)00406-X.

Augland, L.E., Ryabov, V.V., Vernikovsky, V.A., Planke, S., Polozov, A.G., Callegaro, S., Jerram, D.A., and Svensen, H.H., 2019, The main pulse of the Siberian Traps expanded in size and composition: Scientific Reports, v. 9, no. 1, 18723, https://doi.org/10.1038/s41598-019-54023-2.

Beckman, V., Möller, C., Söderlund, U., Corfu, F., Pallon, J., and Chamberlain, K.R., 2014, Metamorphic zircon formation at the transition from gabbro to eclogite in Trollheimen–Surnadalen, Norwegian Caledonides, *in* Corfu, F., Gasser, D., and Chew, D.M., eds., New Perspectives on the Caledonides of Scandinavia and Related Areas: Geological Society, London, Special Publication 390, p. 403–424, https://doi.org/10.1144/SP390.26.

Bell, E.A., Boehnke, P., Barboni, M., and Harrison, T.M., 2019, Tracking chemical alteration in magmatic zircon using rare earth element abundances: Chemical Geology, v. 510, p. 56–71, https://doi.org/10.1016/j.chemgeo.2019.02.027.

Black, L.P., Kamo, S.L., Allen, C.M., Aleinikoff, J.N., Davis, D.W., Korsch, R.J., and Foudoulis, C., 2003, TEMORA 1: A new zircon standard for Phanerozoic U-Pb geochronology: Chemical Geology, v. 200, p. 155–170, https://doi.org/10.1016/S0009-2541(03)00165-7.

Bowring, J.F., McLean, N.M., and Bowring, S.A., 2011, Engineering cyber infrastructure for U-Pb geochronology: Tripoli and U-Pb redux: Geochemistry, Geophysics, Geosystems, v. 12, https://doi.org/10.1029/2010GC003479.

Bowring, S.A., Williams, I.S., and Compston, W., 1989, 3.96 Ga gneisses from the Slave province, Northwest Territories, Canada: Geology, v. 17, p. 971–975, https://doi.org/10.1130/0091-7613(1989)017<0971:GGFTSP>2.3.CO;2.

Burgess, S.D., Bowring, S., and Shen, S.-z., 2014, High-precision timeline for Earth's most severe extinction: Proceedings of the National Academy of Sciences of the United States of America, v. 111, no. 9, p. 3316–3321, https://doi.org/10.1073/pnas.1317692111.

Chamberlain, K.R., and Bowring, S.A., 2001, Apatite-feldspar U-Pb thermochronometer: A reliable mid-range (~450 °C), diffusion controlled system: Chemical Geology, v. 172, no. 1–2, p. 173–200, https://doi.org/10.1016/S0009-2541(00)00242-4.

Chelle-Michou, C., Chiaradia, M., Ovtcharova, M., Ulianov, A., and Wotzlaw, J.-F., 2014, Zircon petrochronology reveals the temporal link between porphyry systems and the magmatic evolution of their hidden plutonic roots (the Eocene Coroccohuayco deposit, Peru): Lithos, v. 198–199, p. 129–140, https://doi.org/10.1016/j.lithos.2014.03.017.

Claiborne, L., Miller, C., and Wooden, J., 2010, Trace element composition of igneous zircon: A thermal and compositional record of the accumulation and evolution of a large silicic batholith, Spirit Mountain, Nevada: Contributions to Mineralogy and Petrology, v. 160, p. 511–531, https://doi.org/10.1007/s00410-010-0491-5.

Compston, W., Williams, I.S., and Meyer, C., 1984, U-Pb Geochronology of zircons from lunar breccia 73217 using a sensitive high mass-resolution ion microprobe: Journal of Geophysical Research: Solid Earth, v. 89, no. S2, p. B525–B534, https://doi.org/10.1029/JB089iS02p0B525.

Condon, D., Schoene, B., McLean, N., Bowring, S., and Parrish, R., 2015, Metrology and traceability of U–Pb isotope dilution geochronology (EARTHTIME Tracer Calibration Part I): Geochimica et Cosmochimica Acta, v. 164, p. 464–480, https://doi.org/10.1016/j.gca.2015.05.026.

Condon, D.J., McLean, N.M., Schoene, B., Bowring, S.A., Parrish, R.R., and Noble, S.R., 2008, Synthetic U-Pb 'standard' solutions for ID-TIMS geochronology [abstract]: Geochimica et Cosmochimica Acta, v. 72, no. 12, Supplement, p. A175–A175.

Corfu, F., 2013, A century of U-Pb geochronology: The long quest towards concordance: Geological Society of America Bulletin, v. 125, p. 33–47, https://doi.org/10.1130/B30698.1.

Corfu, F., Hanchar, J.M., Hoskin, P.W.O., and Kinny, P., 2003, Atlas of zircon textures, *in* Hanchar, J.M., and Hoskin, P.W.O., eds., Zircon: Mineralogical Society of America Reviews in Mineralogy and Geochemistry 53, p. 469–502, https://doi.org/10.1515/9781501509322-019.

Cowan, G.A., and Adler, H.H., 1976, Variability of natural abundance of ^{235}U: Geochimica et Cosmochimica Acta, v. 40, no. 12, p. 1487–1490, https://doi.org/10.1016/0016-7037(76)90087-9.

Crowley, J.L., Schoene, B., and Bowring, S.A., 2007, U-Pb dating of zircon in the Bishop Tuff at the millennial scale: Geology, v. 35, p. 1123–1126, https://doi.org/10.1130/G24017A.1.

Curry, A., Gaynor, S.P., Davies, J., Ovtcharova, M., Simpson, G., and Caricchi, L., 2021, Timescales and thermal evolution of large silicic magma reservoirs during an ignimbrite flare-up: Perspectives from zircon: Contributions to Mineralogy and Petrology, v. 176, 103, https://doi.org/10.1007/s00410-021-01862-w.

Davis, D.W., Krogh, T.E., and Williams, I.S., 2003, Historical development of zircon geochronology: Reviews in Mineralogy and Geochemistry, v. 53, no. 1, p. 145–181, https://doi.org/10.2113/0530145.

Davydov, V.I., Crowley, J.L., Schmitz, M.D., and Poletaev, V.I., 2010, High-precision U-Pb zircon age calibration of the global Carboniferous time scale and Milankovitch band cyclicity in the Donets Basin, eastern Ukraine: Geochemistry, Geophysics, Geosystems, v. 11, https://doi.org/10.1029/2009GC002736.

Deering, C.D., Keller, B., Schoene, B., Bachmann, O., Beane, R., and Ovtcharova, M., 2016, Zircon record of the plutonic-volcanic connection and protracted rhyolite melt evolution: Geology, v. 44, p. 267–270, https://doi.org/10.1130/G37539.1.

DesOrmeau, J.W., Gordon, S.M., Little, T.A., Bowring, S.A., Schoene, B., Samperton, K.M., and Kylander-Clark, A.R.C., 2018, Using eclogite retrogression to track the rapid exhumation of the Pliocene Papua New Guinea UHP Terrane: Journal of Petrology, v. 59, p. 2017–2042, https://doi.org/10.1093/petrology/egy088.

Eberth, D.A., and Kamo, S.L., 2020, High-precision U–Pb CA–ID–TIMS dating and chronostratigraphy of the dinosaur-rich Horseshoe Canyon Formation (Upper Cretaceous, Campanian–Maastrichtian), Red Deer River Valley, Alberta, Canada: Canadian Journal of Earth Sciences, v. 57, no. 10, p. 1220–1237, https://doi.org/10.1139/cjes-2019-0019.

Eddy, M.P., Ibañez-Mejia, M., Burgess, S.D., Coble, M.A., Cordani, U.G., DesOrmeau, J., Gehrels, G.E., Li, X., MacLennan, S., and Pecha, M., 2019, GHR 1 zircon–A new Eocene natural reference material for microbeam U-Pb geochronology and Hf isotopic analysis of zircon: Geostandards and Geoanalytical Research, v. 43, no. 1, p. 113–132, https://doi.org/10.1111/ggr.12246.

Eddy, M.P., Schoene, B., Samperton, K.M., Keller, G., Adatte, T., and Khadri, S.F., 2020, U-Pb zircon age constraints on the earliest eruptions of the Deccan Large Igneous Province, Malwa Plateau, India: Earth and Planetary Science Letters, v. 540, https://doi.org/10.1016/j.epsl.2020.116249.

Galeotti, S., Sahy, D., Agnini, C., Condon, D., Fornaciari, E., Francescone, F., Giusberti, L., Pälike, H., Spofforth, D.J.A., and Rio, D., 2019, Astrochronology and radioisotopic dating of the Alano di Piave section (NE Italy), candidate GSSP for the Priabonian Stage (late Eocene): Earth and Planetary Science Letters, v. 525, https://doi.org/10.1016/j.epsl.2019.115746.

Gaynor, S.P., Ruiz, M., and Schaltegger, U., 2022a, The importance of high precision in the evaluation of U-Pb zircon age spectra: Chemical Geology, v. 603, https://doi.org/10.1016/j.chemgeo.2022.120913.

Gaynor, S.P., Svensen, H.H., Polteau, S., and Schaltegger, U., 2022b, Local melt contamination and global climate impact: Dating the emplacement of Karoo LIP sills into organic-rich shale: Earth and Planetary Science Letters, v. 579, https://doi.org/10.1016/j.epsl.2022.117371.

Gaynor, S.P., Smith, T.M., and Schaltegger, U., 2023, Tracing magmatic genesis and evolution through single zircon crystals from successive supereruptions from the Socorro Caldera Complex, USA: Earth and Planetary Science Letters, v. 616, https://doi.org/10.1016/j.epsl.2023.118236.

Gerstenberger, H., and Haase, G., 1997, A highly effective emitter substance for mass spectrometric Pb isotope ratio determinations: Chemical Geology, v. 136, p. 309–312, https://doi.org/10.1016/S0009-2541(96)00033-2.

Glazner, A.F., and Sadler, P.M., 2016, Estimating the duration of geologic intervals from a small number of age determinations: A challenge common to petrology and paleobiology: Geochemistry, Geophysics, Geosystems, v. 17, no. 12, p. 4892–4898, https://doi.org/10.1002/2016GC006542.

Gordon, S.M., Bowring, S.A., Whitney, D.L., Miller, R.B., and McLean, N., 2010, Time scales of metamorphism, deformation, and crustal melting in a continental arc, North Cascades USA: Geological Society of America Bulletin, v. 122, p. 1308–1330, https://doi.org/10.1130/B30060.1.

Gradstein, F.M., Ogg, J.G., Schmitz, M.D., and Ogg, G.M., 2020, Geologic Time Scale 2020: Elsevier.

Griffis, N.P., Mundil, R., Montañez, I.P., Isbell, J., Fedorchuk, N., Vesely, F., Iannuzzi, R., and Yin, Q.-Z., 2018, A new stratigraphic framework built on U-Pb single-zircon TIMS ages and implications for the timing of the penultimate icehouse (Paraná Basin, Brazil): Geological Society of America Bulletin, v. 130, p. 848–858, https://doi.org/10.1130/B31775.1.

Griffis, N.P., Montañez, I.P., Mundil, R., Richey, J., Isbell, J., Fedorchuk, N., Linol, B., Iannuzzi, R., Vesely, F., Mottin, T., da Rosa, E., Keller, B., and Yin, Q.-Z., 2019, Coupled stratigraphic and U-Pb zircon age constraints on the late Paleozoic icehouse-to-greenhouse turnover in south-central Gondwana: Geology, v. 47, p. 1146–1150, https://doi.org/10.1130/G46740.1.

Hawkins, D.P., and Bowring, S.A., 1997, U-Pb systematics of monazite and xenotime: Case studies from the Paleoproterozoic of the Grand Canyon, Arizona: Contributions to Mineralogy and Petrology, v. 127, p. 87–103, https://doi.org/10.1007/s004100050267.

Hayden, L., Watson, E., and Wark, D., 2008, A thermobarometer for sphene (titanite): Contributions to Mineralogy and Petrology, v. 155, no. 4, p. 529–540, https://doi.org/10.1007/s00410-007-0256-y.

Hiess, J., Condon, D.J., McLean, N., and Noble, S.R., 2012, $^{238}U/^{235}U$ systematics in terrestrial uranium-bearing minerals: Science, v. 335, no. 6076, p. 1610–1614, https://doi.org/10.1126/science.1215507.

Horstwood, M.S.A., Košler, J., Gehrels, G., Jackson, S.E., McLean, N.M., Paton, C., Pearson, N.J., Sircombe, K., Sylvester, P., Vermeesch, P., Bowring, J.F., Condon, D.J., and Schoene, B., 2016, Community-derived standards for LA-ICP-MS U-Th-Pb geochronology—Uncertainty propagation, age interpretation and data reporting: Geostandards and Geoanalytical Research, v. 40, p. 311–332, https://doi.org/10.1111/j.1751-908X.2016.00379.x.

Huyskens, M.H., Zink, S., and Amelin, Y., 2016, Evaluation of temperature-time conditions for the chemical abrasion treatment of single zircons for U–Pb geochronology: Chemical Geology, v. 438, p. 25–35, https://doi.org/10.1016/j.chemgeo.2016.05.013.

Ickert, R.B., Mundil, R., Magee, C.W., and Mulcahy, S.R., 2015, The U–Th–Pb systematics of zircon from the Bishop Tuff: A case study in challenges to high-precision Pb/U geochronology at the millennial scale: Geochimica et Cosmochimica Acta, v. 168, p. 88–110, https://doi.org/10.1016/j.gca.2015.07.018.

Inghram, M.G., 1954, Stable isotope dilution as an analytical tool: Annual Review of Nuclear Science, v. 4, no. 1, p. 81–92, https://doi.org/10.1146/annurev.ns.04.120154.000501.

Jaffey, A.H., Flynn, K.F., Glendenin, L.E., Bentley, W.C., and Essling, A.M., 1971, Precision measurement of half-lives and specific activities of ^{235}U and ^{238}U: Physical Review, v. C4, p. 1889–1906.

Kasbohm, J., and Schoene, B., 2018, Rapid eruption of the Columbia River flood basalt and correlation with the mid-Miocene climate optimum: Science Advances, v. 4, no. 9, https://doi.org/10.1126/sciadv.aat8223.

Downloaded from http://pubs.geoscienceworld.org/gsa/gsabulletin/article-pdf/136/9-10/4233/6898541/b37321.1.pdf
by guest

Keller, C.B., Schoene, B., and Samperton, K.M., 2018, A stochastic sampling approach to zircon eruption age interpretation: Geochemical Perspectives Letters, v. 8, p. 31–35, https://doi.org/10.7185/geochemlet.1826.

Keller, C.B., Boehnke, P., Schoene, B., and Harrison, T.M., 2019, Stepwise chemical abrasion ID-TIMS-TEA of microfractured Hadean zircon: Geochronology, v. 2019, p. 1–20.

Kelly, N.M., and Harley, S.L., 2005, An integrated microtextural and chemical approach to zircon geochronology: Refining the Archaean history of the Napier Complex, east Antarctica: Contributions to Mineralogy and Petrology, v. 149, p. 57–84, https://doi.org/10.1007/s00410-004-0635-6.

Kennedy, A.K., Wotzlaw, J.-F., Schaltegger, U., Crowley, J.L., and Schmitz, M.D., 2014, Eocene zircon reference material for microanalysis of U-Th-Pb isotopes and trace elements: Canadian Mineralogist, v. 52, p. 409–421, https://doi.org/10.3749/canmin.52.3.409.

Klein, B.Z., and Eddy, M.P., 2023, What's in an age?: Calculation and interpretation of ages and durations from U-Pb zircon geochronology of igneous rocks: Geological Society of America Bulletin, v. 136, p. 93–109, https://doi.org/10.1130/B36686.1.

Kohn, M.J., 2016, Metamorphic chronology—A tool for all ages: Past achievements and future prospects: The American Mineralogist, v. 101, p. 25–42, https://doi.org/10.2138/am-2016-5146.

Kohn, M.J., Engi, M., and Lanari, P., eds., 2017, Petrochronology: Methods and Applications: Mineralogical Society of America Reviews in Mineralogy and Geochemistry 83: De Gruyter, 575 p., https://doi.org/10.1515/9783110561890.

Krogh, T.E., 1973, A low contamination method for hydrothermal decomposition of zircon and extraction of U and Pb for isotopic age determination: Geochimica et Cosmochimica Acta, v. 37, p. 485–494, https://doi.org/10.1016/0016-7037(73)90213-5.

Krogh, T.E., and Davis, D.W., 1975, The production and preparation of ^{205}Pb for use as a tracer for isotope dilution analyses: Carnegie Institution of Washington Yearbook 74, p. 416–417.

Liao, S., Huyskens, M.H., Yin, Q.-Z., and Schmitz, B., 2020, Absolute dating of the L-chondrite parent body breakup with high-precision U–Pb zircon geochronology from Ordovician limestone: Earth and Planetary Science Letters, v. 547, https://doi.org/10.1016/j.epsl.2020.116442.

Ling, X.-X., Huyskens, M.H., Li, Q.-L., Yin, Q.-Z., Werner, R., Liu, Y., Tang, G.-Q., Yang, Y.-N., and Li, X.-H., 2017, Monazite RW-1: A homogenous natural reference material for SIMS U–Pb and Th–Pb isotopic analysis: Mineralogy and Petrology, v. 111, no. 2, p. 163–172, https://doi.org/10.1007/s00710-016-0478-7.

Livermore, B.D., Connelly, J.N., Moynier, F., and Bizzarro, M., 2018, Evaluating the robustness of a consensus ^{238}U/^{235}U value for U-Pb geochronology: Geochimica et Cosmochimica Acta, v. 237, p. 171–183, https://doi.org/10.1016/j.gca.2018.06.014.

Ludwig, K.R., 1991, Isoplot—A plotting and regression program for radiogenic isotope data: USGS Open-File Report 91-445.

Ludwig, K.R., 1998, On the treatment of concordant uranium-lead ages: Geochimica et Cosmochimica Acta, v. 62, no. 4, p. 665–676, https://doi.org/10.1016/S0016-7037(98)00059-3.

Mackinder, A., Cousens, B.L., Ernst, R.E., and Chamberlain, K.R., 2019, Geochemical, isotopic, and U–Pb zircon study of the central and southern portions of the 780 Ma Gunbarrel Large Igneous Province in western Laurentia: Canadian Journal of Earth Sciences, v. 56, no. 7, p. 738–755, https://doi.org/10.1139/cjes-2018-0083.

Mattinson, J.M., 2000, Revising the "gold standard"—The uranium decay constants of Jaffey et al., 1971: Abstract V61A-02 presented at 2000 Fall Meeting, AGU, San Francisco, California, 15–19 December.

Mattinson, J.M., 2005, Zircon U-Pb chemical-abrasion ("CA-TIMS") method: Combined annealing and multi-step dissolution analysis for improved precision and accuracy of zircon ages: Chemical Geology, v. 220, no. 1–2, p. 47–56.

Mattinson, J.M., 2010, Analysis of the relative decay constants of ^{235}U and ^{238}U by multi-step CA-TIMS measurements of closed-system natural zircon samples: Chemical Geology, v. 275, no. 3–4, p. 186–198.

Mattinson, J.M., 2011, Extending the Krogh legacy: Development of the CA-TIMS method for zircon U-Pb geochronology: Canadian Journal of Earth Sciences, v. 48, no. 2, p. 95–105, https://doi.org/10.1139/E10-023.

Mattinson, J.M., 2013, Revolution and evolution: 100 years of U–Pb geochronology: Elements, v. 9, no. 1, p. 53–57, https://doi.org/10.2113/gselements.9.1.53.

McKanna, A.J., Koran, I., Schoene, B., and Ketcham, R.A., 2023, Chemical abrasion: The mechanics of zircon dissolution: Geochronology, v. 5, no. 1, p. 127–151, https://doi.org/10.5194/gchron-5-127-2023.

McKanna, A.J., Schoene, B., and Szymanowski, D., 2024, Geochronological and geochemical effects of zircon chemical abrasion: Insights from single-crystal stepwise dissolution experiments: Geochronology, v. 6, no. 1, p. 1–20, https://doi.org/10.5194/gchron-6-1-2024.

McLean, N.M., Bowring, J.F., and Bowring, S.A., 2011, An algorithm for U-Pb isotope dilution data reduction and uncertainty propagation: Geochemistry, Geophysics, Geosystems, v. 12, https://doi.org/10.1029/2010GC003478.

McLean, N.M., Condon, D.J., Schoene, B., and Bowring, S.A., 2015, Evaluating uncertainties in the calibration of isotopic reference materials and multi-element isotopic tracers (EARTHTIME Tracer Calibration Part II): Geochimica et Cosmochimica Acta, v. 164, p. 481–501, https://doi.org/10.1016/j.gca.2015.02.040.

Min, K., Mundil, R., Renne, P.R., and Ludwig, K.R., 2000, A test for systematic errors in ^{40}Ar/^{39}Ar geochronology through comparison with U-Pb analysis of a 1.1 Ga rhyolite: Geochimica et Cosmochimica Acta, v. 64, p. 73–98, https://doi.org/10.1016/S0016-7037(99)00204-5.

Mundil, R., Ludwig, K.R., Metcalfe, I., and Renne, P.R., 2004, Age and timing of the Permian mass extinctions: U/Pb dating of closed-system zircons: Science, v. 305, no. 5691, p. 1760–1763, https://doi.org/10.1126/science.1101012.

Mungall, J.E., Kamo, S.L., and McQuade, S., 2016, U–Pb geochronology documents out-of-sequence emplacement of ultramafic layers in the Bushveld Igneous Complex of South Africa: Nature Communications, v. 7, no. 1, https://doi.org/10.1038/ncomms13385.

Nasdala, L., Corfu, F., Schoene, B., Tapster, S.R., Wall, C.J., Schmitz, M.D., Ovtcharova, M., Schaltegger, U., Kennedy, A.K., Kronz, A., Reiners, P.W., Yang, Y.-H., Wu, F.-Y., Gain, S.E.M., Griffin, W.L., Szymanowski, D., Chanmuang, N.C., Ende, M., Valley, J.W., Spicuzza, M.J., Wanthanachaisaeng, B., and Giester, G., 2018, GZ7 and GZ8—Two zircon reference materials for SIMS U-Pb geochronology: Geostandards and Geoanalytical Research, v. 42, no. 4, p. 431–457, https://doi.org/10.1111/ggr.12239.

Nebel, O., Scherer, E.E., and Mezger, K., 2010, Evaluation of the ^{87}Rb decay constant by age comparison against the U-Pb system: Earth and Planetary Science Letters, v. 301, no. 1–2, p. 1–8.

Newman, E., Bell, W.A., Davis, W.C., Love, L.O., Prater, W.K., Spainhour, K.A., Tracy, J.G., and Veach, A.M., 1976, Some new techniques and recent developments in isotope separations at Oak Ridge: Nuclear Instruments and Methods, v. 139, p. 87–93, https://doi.org/10.1016/0029-554X(76)90660-1.

Neymark, L.A., Amelin, Y.V., and Paces, J.B., 2000, ^{206}Pb–^{230}Th–^{234}U–^{238}U and ^{207}Pb–^{235}U geochronology of Quaternary opal, Yucca Mountain, Nevada: Geochimica et Cosmochimica Acta, v. 64, no. 17, p. 2913–2928, https://doi.org/10.1016/S0016-7037(00)00408-7.

O'Connor, L., Szymanowski, D., Eddy, M.P., Samperton, K.M., and Schoene, B., 2022, A red bole zircon record of cryptic silicic volcanism in the Deccan Traps, India: Geology, v. 50, p. 460–464, https://doi.org/10.1130/G49613.1.

Ovtcharova, M., Goudemand, N., Hammer, Ø., Guodun, K., Cordey, F., Galfetti, T., Schaltegger, U., and Bucher, H., 2015, Developing a strategy for accurate definition of a geological boundary through radio-isotopic and biochronological dating: The Early–Middle Triassic boundary (South China): Earth-Science Reviews, v. 146, p. 65–76, https://doi.org/10.1016/j.earscirev.2015.03.006.

Pamukçu, A.S., Schoene, B., Deering, C.D., Keller, C.B., and Eddy, M.P., 2022, Volcano-pluton connections at the Lake City magmatic center (Colorado, USA): Geosphere, v. 18, p. 1435–1452, https://doi.org/10.1130/GES02467.1.

Parrish, R.R., 1990, U-Pb dating of monazite and its application to geological problems: Canadian Journal of Earth Sciences, v. 27, p. 1431–1450, https://doi.org/10.1139/e90-152.

Parrish, R.R., and Krogh, T.E., 1987, Synthesis and purification of ^{205}Pb for U-Pb geochronology: Chemical Geology, v. 66, no. 1–2, p. 103–110.

Parrish, R.R., and Noble, S.R., 2003, Zircon U-Th-Pb geochronology by isotope dilution–thermal ionization mass spectrometry (ID-TIMS): Reviews in Mineralogy and Geochemistry, v. 53, no. 1, p. 183–213, https://doi.org/10.2113/0530183.

Parsons-Davis, T., Wimpenny, J., Keller, C.B., Thomas, K., Samperton, K.M., Renne, P.R., Mundil, R., Moody, K., Knight, K., and Kristo, M.J., 2018, New measurement of the ^{238}U decay constant with inductively coupled plasma mass spectrometry: Journal of Radioanalytical and Nuclear Chemistry, v. 318, no. 1, p. 711–721, https://doi.org/10.1007/s10967-018-6148-y.

Paul, A.N., Spikings, R.A., and Gaynor, S.P., 2021, U-Pb ID-TIMS reference ages and initial Pb isotope compositions for Durango and Wilberforce apatites: Chemical Geology, v. 586, https://doi.org/10.1016/j.chemgeo.2021.120604.

Peterman, E.M., Mattinson, J.M., and Hacker, B.R., 2012, Multi-step TIMS and CA-TIMS monazite U-Pb geochronology: Chemical Geology, v. 312–313, p. 58–73, https://doi.org/10.1016/j.chemgeo.2012.04.006.

Piccoli, F., Rubatto, D., Ovtcharova, M., Hermann, J., Guillong, M., and Vitale Brovarone, A., 2023, Dating fluid infiltration and deformation in the subducted ultramafic oceanic lithosphere by perovskite geochronology: Chemical Geology, v. 615, https://doi.org/10.1016/j.chemgeo.2022.121205.

Quinn, D., Linzmeier, B., Sundell, K., Gehrels, G., Goring, S., Marcott, S., Meyers, S., Peters, S., Ross, J., and Schmitz, M., Implementing the Sparrow laboratory data system in multiple subdomains of geochronology and geochemistry: Proceedings of the EGU General Assembly Conference Abstracts 2021, p. EGU21-13832.

Ramezani, J., Schmitz, M.D., Davydov, V.I., Bowring, S.A., Snyder, W.S., and Northrup, C.J., 2007, High-precision U-Pb zircon age constraints on the Carboniferous–Permian boundary in the southern Urals stratotype: Earth and Planetary Science Letters, v. 256, no. 1–2, p. 244–257, https://doi.org/10.1016/j.epsl.2007.01.032.

Ramezani, J., Beveridge, T.L., Rogers, R.R., Eberth, D.A., and Roberts, E.M., 2022, Calibrating the zenith of dinosaur diversity in the Campanian of the Western Interior Basin by CA-ID-TIMS U–Pb geochronology: Scientific Reports, v. 12, 16026, https://doi.org/10.1038/s41598-022-19896-w.

Ratschbacher, B.C., Keller, C.B., Schoene, B., Paterson, S.R., Anderson, J.L., Okaya, D., Putirka, K., and Lippoldt, R., 2018, A new workflow to assess emplacement duration and melt residence time of compositionally diverse magmas emplaced in a sub-volcanic reservoir: Journal of Petrology, v. 59, no. 9, p. 1787–1809, https://doi.org/10.1093/petrology/egy079.

Reid, M., Vazquez, J., and Schmitt, A., 2011, Zircon-scale insights into the history of a Supervolcano, Bishop Tuff, Long Valley, California, with implications for the Ti-in-zircon geothermometer: Contributions to Mineralogy and Petrology, v. 161, p. 293–311, https://doi.org/10.1007/s00410-010-0532-0.

Reiners, P.W., Carlson, R.W., Renne, P.R., Cooper, K.M., Granger, D.E., McLean, N.M., and Schoene, B., 2017, Geochronology and Thermochronology: John Wiley and Sons, https://doi.org/10.1002/9781118455876.

Renne, P.R., Karner, D.B., and Ludwig, K.R., 1998, Absolute ages aren't exactly: Science, v. 282, p. 1840–1841, https://doi.org/10.1126/science.282.5395.1840.

Renne, P.R., Mundil, R., Balco, G., Min, K., and Ludwig, K.R., 2010, Joint determination of 40 K decay constants and ^{40}Ar*/^{40}K for the Fish Canyon sanidine standard, and improved accuracy for ^{40}Ar/^{39}Ar geo-

Downloaded from http://pubs.geoscienceworld.org/gsa/gsabulletin/article-pdf/136/9-10/4233/6898541/b37321.1.pdf
by guest

chronology: Geochimica et Cosmochimica Acta, v. 74, no. 18, p. 5349–5367.
Richter, S., Alonso-Munoz, A., Eykens, R., Jacobsson, U., Kuehn, H., Verbruggen, A., Aregbe, Y., Wellum, R., and Keegan, E., 2008, The isotopic composition of natural uranium samples—Measurements using the new $n(^{233}U)/n(^{236}U)$ double spike IRMM-3636: International Journal of Mass Spectrometry, v. 269, no. 1–2, p. 145–148, https://doi.org/10.1016/j.ijms.2007.09.012.
Rioux, M., Bowring, S., Dudás, F., and Hanson, R., 2010, Characterizing the U–Pb systematics of baddeleyite through chemical abrasion: Application of multi-step digestion methods to baddeleyite geochronology: Contributions to Mineralogy and Petrology, v. 160, no. 5, p. 777–801, https://doi.org/10.1007/s00410-010-0507-1.
Rioux, M., Johan Lissenberg, C., McLean, N.M., Bowring, S.A., MacLeod, C.J., Hellebrand, E., and Shimizu, N., 2012, Protracted timescales of lower crustal growth at the fast-spreading East Pacific Rise: Nature Geoscience, v. 5, no. 4, p. 275–278, https://doi.org/10.1038/ngeo1378.
Rioux, M., Bowring, S., Cheadle, M., and John, B., 2015, Evidence for initial excess ^{231}Pa in mid-ocean ridge zircons: Chemical Geology, v. 397, p. 143–156, https://doi.org/10.1016/j.chemgeo.2015.01.011.
Rivera, T.A., Storey, M., Schmitz, M.D., and Crowley, J.L., 2013, Age intercalibration of $^{40}Ar/^{39}Ar$ sanidine and chemically distinct U/Pb zircon populations from the Alder Creek Rhyolite Quaternary geochronology standard: Chemical Geology, v. 345, p. 87–98, https://doi.org/10.1016/j.chemgeo.2013.02.021.
Rivera, T.A., Schmitz, M.D., Crowley, J.L., and Storey, M., 2014, Rapid magma evolution constrained by zircon petrochronology and $^{40}Ar/^{39}Ar$ sanidine ages for the Huckleberry Ridge Tuff, Yellowstone, USA: Geology, v. 42, p. 643–646, https://doi.org/10.1130/G35808.1.
Sageman, B.B., Singer, B.S., Meyers, S.R., Siewert, S.E., Walaszczyk, I., Condon, D.J., Jicha, B.R., Obradovich, J.D., and Sawyer, D.A., 2014, Integrating $^{40}Ar/^{39}Ar$, U-Pb, and astronomical clocks in the Cretaceous Niobrara Formation, Western Interior Basin, USA: Geological Society of America Bulletin, v. 126, p. 956–973, https://doi.org/10.1130/B30929.1.
Sahy, D., Condon, D.J., Hilgen, F.J., and Kuiper, K.F., 2017, Reducing disparity in radio-isotopic and astrochronology-based time scales of the late Eocene and Oligocene: Paleoceanography, v. 32, no. 10, p. 1018–1035, https://doi.org/10.1002/2017PA003197.
Sambridge, M., and Compston, W., 1994, Mixture modeling of multi-component data sets with application to ion-probe zircon ages: Earth and Planetary Science Letters, v. 128, no. 3–4, p. 373–390, https://doi.org/10.1016/0012-821X(94)90157-0.
Samperton, K.M., Schoene, B., Cottle, J.M., Brenhin Keller, C., Crowley, J.L., and Schmitz, M.D., 2015, Magma emplacement, differentiation and cooling in the middle crust: Integrated zircon geochronological–geochemical constraints from the Bergell Intrusion, Central Alps: Chemical Geology, v. 417, p. 322–340, https://doi.org/10.1016/j.chemgeo.2015.10.024.
Samperton, K.M., Bell, E.A., Barboni, M., Keller, C.B., and Schoene, B., 2017, Zircon age-temperature-compositional spectra in plutonic rocks: Geology, v. 45, p. 983–986, https://doi.org/10.1130/G38645.1.
Santos, M.M., Lana, C., Scholz, R., Buick, I., Schmitz, M.D., Kamo, S.L., Gerdes, A., Corfu, F., Tapster, S., Lancaster, P., Storey, C.D., Basei, M.A.S., Tohver, E., Alkmim, A., Nalini, H., Krambrock, K., Fantini, C., and Wiedenbeck, M., 2017, A new appraisal of Sri Lankan BB zircon as a reference material for LA-ICP-MS U-Pb geochronology and Lu-Hf isotope tracing: Geostandards and Geoanalytical Research, v. 41, no. 3, p. 335–358, https://doi.org/10.1111/ggr.12167.
Schaen, A.J., Schoene, B., Dufek, J., Singer, B.S., Eddy, M.P., Jicha, B.R., and Cottle, J.M., 2021, Transient rhyolite melt extraction to produce a shallow granitic pluton: Science Advances, v. 7, no. 21, https://doi.org/10.1126/sciadv.abf0604.
Schaltegger, U., and Davies, J.H., 2017, Petrochronology of zircon and baddeleyite in igneous rocks: Reconstructing magmatic processes at high temporal resolution: Reviews in Mineralogy and Geochemistry, v. 83, no. 1, p. 297–328, https://doi.org/10.2138/rmg.2017.83.10.
Schaltegger, U., Zeilinger, G., Frank, M., and Burg, J.P., 2002, Multiple mantle sources during island arc magmatism: U–Pb and Hf isotopic evidence from the Kohistan arc complex, Pakistan: Terra Nova, v. 14, no. 6, p. 461–468, https://doi.org/10.1046/j.1365-3121.2002.00432.x.
Schaltegger, U., Schmitt, A.K., and Horstwood, M.S.A., 2015, U–Th–Pb zircon geochronology by ID-TIMS, SIMS, and laser ablation ICP-MS: Recipes, interpretations, and opportunities: Chemical Geology, v. 402, p. 89–110, https://doi.org/10.1016/j.chemgeo.2015.02.028.
Schaltegger, U., Ovtcharova, M., Gaynor, S.P., Schoene, B., Wotzlaw, J.-F., Davies, J.F., Farina, F., Greber, N.D., Szymanowski, D., and Chelle-Michou, C., 2021, Long-term repeatability and interlaboratory reproducibility of high-precision ID-TIMS U–Pb geochronology: Journal of Analytical Atomic Spectrometry, v. 36, no. 7, p. 1466–1477, https://doi.org/10.1039/D1JA00116G.
Schärer, U., 1984, The effect of initial ^{230}Th disequilibrium on young U-Pb ages: The Makalu case, Himalaya: Earth and Planetary Science Letters, v. 67, p. 191–204, https://doi.org/10.1016/0012-821X(84)90114-6.
Schmitt, A., Danišík, M., Evans, N., Siebel, W., Kiemele, E., Aydin, F., and Harvey, J., 2011, Acigöl rhyolite field, Central Anatolia (part 1): High-resolution dating of eruption episodes and zircon growth rates: Contributions to Mineralogy and Petrology, v. 162, no. 6, p. 1215–1231, https://doi.org/10.1007/s00410-011-0648-x.
Schmitt, A.K., 2007, Ion microprobe analysis of $(^{231}Pa)/(^{235}U)$ and an appraisal of protactinium partitioning in igneous zircon: The American Mineralogist, v. 92, no. 4, p. 691–694, https://doi.org/10.2138/am.2007.2449.
Schmitz, M.D., and Bowring, S.A., 2001, U-Pb zircon and titanite systematics of the Fish Canyon Tuff: An assessment of high-precision U-Pb geochronology and its application to young volcanic rocks: Geochimica et Cosmochimica Acta, v. 65, no. 15, p. 2571–2587, https://doi.org/10.1016/S0016-7037(01)00616-0.
Schmitz, M.D., and Kuiper, K.F., 2013, High-precision geochronology: Elements, v. 9, no. 1, p. 25–30, https://doi.org/10.2113/gselements.9.1.25.
Schmitz, M.D., and Schoene, B., 2007, Derivation of isotope ratios, errors, and error correlations for U-Pb geochronology using ^{205}Pb-^{235}U-(^{233}U)-spiked isotope dilution thermal ionization mass spectrometric data: Geochemistry, Geophysics, Geosystems, v. 8, no. 8, https://doi.org/10.1029/2006GC001492.
Schoene, B., 2014, U-Th-Pb geochronology, *in* Rudnick, R., ed., Treatise on Geochemistry, Volume 4: Elsevier, p. 341–378, https://doi.org/10.1016/B978-0-08-095975-7.00310-7.
Schoene, B., and Baxter, E.F., 2017, Petrochronology and TIMS: Reviews in Mineralogy and Geochemistry, v. 83, no. 1, p. 231–260, https://doi.org/10.2138/rmg.2017.83.8.
Schoene, B., Crowley, J.L., Condon, D.C., Schmitz, M.D., and Bowring, S.A., 2006, Reassessing the uranium decay constants for geochronology using ID-TIMS U-Pb data: Geochimica et Cosmochimica Acta, v. 70, p. 426–445, https://doi.org/10.1016/j.gca.2005.09.007.
Schoene, B., Guex, J., Bartolini, A., Schaltegger, U., and Blackburn, T.J., 2010a, Correlating the end-Triassic mass extinction and flood basalt volcanism at the 100,000-year level: Geology, v. 38, p. 387–390, https://doi.org/10.1130/G30683.1.
Schoene, B., Latkoczy, C., Schaltegger, U., and Gunther, D., 2010b, A new method integrating high-precision U-Pb geochronology with zircon trace element analysis (U-Pb TIMS-TEA): Geochimica et Cosmochimica Acta, v. 74, no. 24, p. 7144–7159, https://doi.org/10.1016/j.gca.2010.09.016.
Schoene, B., Schaltegger, U., Brack, P., Latkoczy, C., Stracke, A., and Günther, D., 2012, Rates of magma differentiation and emplacement in a ballooning pluton recorded by U-Pb TIMS-TEA, Adamello batholith, Italy: Earth and Planetary Science Letters, v. 355–356, p. 162–173, https://doi.org/10.1016/j.epsl.2012.08.019.
Schoene, B., Samperton, K.M., Eddy, M.P., Keller, G., Adatte, T., Bowring, S.A., Khadri, S.F., and Gertsch, B., 2015, U-Pb geochronology of the Deccan Traps and relation to the end-Cretaceous mass extinction: Science, v. 347, no. 6218, p. 182–184, https://doi.org/10.1126/science.aaa0118.
Scoates, J.S., and Friedman, R.M., 2008, Precise age of the platiniferous Merensky Reef, Bushveld Complex, South Africa, by the U-Pb zircon chemical abrasion ID-TIMS technique: Economic Geology, v. 103, no. 3, p. 465–471, https://doi.org/10.2113/gsecongeo.103.3.465.
Selby, D., Creaser, R.A., Stein, H.J., Markey, R.J., and Hannah, J.L., 2007, Assessment of the ^{187}Re decay constant by cross calibration of Re-Os molybdenite and U-Pb zircon chronometers in magmatic ore systems: Geochimica et Cosmochimica Acta, v. 71, no. 8, p. 1999–2013, https://doi.org/10.1016/j.gca.2007.01.008.
Sláma, J., Kosler, J., Condon, D.J., Crowley, J.L., Gerdes, A., Hanchar, J.M., Horstwood, M.S.A., Morris, G.A., Nasdala, L., Norberg, N., Schaltegger, U., Schoene, B., Tubrett, M.N., and Whitehouse, M.J., 2008, Plesovice zircon–A new natural reference material for U-Pb and Hf isotopic microanalysis: Chemical Geology, v. 249, no. 1–2, p. 1–35, https://doi.org/10.1016/j.chemgeo.2007.11.005.
Stacey, J.C., and Kramers, J.D., 1975, Approximation of terrestrial lead isotope evolution by a two-stage model: Earth and Planetary Science Letters, v. 26, p. 207–221, https://doi.org/10.1016/0012-821X(75)90088-6.
Steiger, R.H., and Jager, E., 1977, Subcommission on Geochronology—Convention on use of decay constants in geochronology and cosmochronology: Earth and Planetary Science Letters, v. 36, no. 3, p. 359–362, https://doi.org/10.1016/0012-821X(77)90060-7.
Steiger, R.H., Bickel, R.A., and Meier, M., 1993, Conventional U-Pb dating of single fragments of zircon for petrogenetic studies of Phanerozoic granitoids: Earth and Planetary Science Letters, v. 115, no. 1–4, p. 197–209, https://doi.org/10.1016/0012-821X(93)90222-U.
Stirling, C.H., Andersen, M.B., Potter, E.K., and Halliday, A.N., 2007, Low-temperature isotopic fractionation of uranium: Earth and Planetary Science Letters, v. 264, no. 1–2, p. 208–225, https://doi.org/10.1016/j.epsl.2007.09.019.
Stracke, A., Scherer, E.E., and Reynolds, B.C., 2014, 15.4—Application of isotope dilution in geochemistry, *in* Turekian, K.K., ed., Treatise on Geochemistry (second edition): Elsevier, p. 71–86, https://doi.org/10.1016/B978-0-08-095975-7.01404-2.
Szymanowski, D., and Schoene, B., 2020, U–Pb ID-TIMS geochronology using ATONA amplifiers: Journal of Analytical Atomic Spectrometry, v. 35, no. 6, p. 1207–1216, https://doi.org/10.1039/D0JA00135J.
Szymanowski, D., Wotzlaw, J.-F., Ellis, B.S., Bachmann, O., Guillong, M., and von Quadt, A., 2017, Protracted near-solidus storage and pre-eruptive rejuvenation of large magma reservoirs: Nature Geoscience, v. 10, no. 10, p. 777–782, https://doi.org/10.1038/ngeo3020.
Tapster, S., Condon, D.J., Naden, J., Noble, S.R., Petterson, M.G., Roberts, N.M.W., Saunders, A.D., and Smith, D.J., 2016, Rapid thermal rejuvenation of high-crystallinity magma linked to porphyry copper deposit formation; evidence from the Koloula Porphyry Prospect, Solomon Islands: Earth and Planetary Science Letters, v. 442, p. 206–217, https://doi.org/10.1016/j.epsl.2016.02.046.
Taylor, R.J.M., Kirkland, C.L., and Clark, C., 2016, Accessories after the facts: Constraining the timing, duration and conditions of high-temperature metamorphic processes: Lithos, v. 264, p. 239–257, https://doi.org/10.1016/j.lithos.2016.09.004.
Tilton, G.R., Patterson, C., Brown, H., Inghram, M., Hayden, R., Hess, D., and Larsen, E., 1955a, Isotopic composition and distribution of lead, uranium and thorium in a Precambrian granite: Geological Society of America Bulletin, v. 66, p. 1131–1148, https://doi.org/10.1130/0016-7606(1955)66[1131:ICADOL]2.0.CO;2.
Tilton, G.R., Patterson, C., Brown, H., Inghram, M., Hayden, R., Hess, D., and Larson, E., 1955b, Isotopic composition and distribution of lead, uranium, and thorium in a Precambrian granite: Geological Society of America

Downloaded from http://pubs.geoscienceworld.org/gsa/gsabulletin/article-pdf/136/9-10/4233/6898541/b37321.1.pdf
by guest

Bulletin, v. 66, p. 1131–1148, https://doi.org/10.1130/0016-7606(1955)66[1131:ICADOL]2.0.CO;2.

Tissot, F.L., and Dauphas, N., 2015, Uranium isotopic compositions of the crust and ocean: Age corrections, U budget and global extent of modern anoxia: Geochimica et Cosmochimica Acta, v. 167, p. 113–143, https://doi.org/10.1016/j.gca.2015.06.034.

Tissot, F.L., Ibanez-Mejia, M., Boehnke, P., Dauphas, N., McGee, D., Grove, T.L., and Harrison, T.M., 2019, $^{238}U/^{235}U$ measurement in single-zircon crystals: Implications for the Hadean environment, magmatic differentiation and geochronology: Journal of Analytical Atomic Spectrometry, v. 34, no. 10, p. 2035–2052, https://doi.org/10.1039/C9JA00205G.

Todt, W., Cliff, R.A., Hanser, A., and Hofmann, A., 1996, Evaluation of a ^{202}Pb–^{205}Pb double spike for high-precision lead isotope analysis, *in* Basu, A., and Hart, S., eds., Earth Processes: Reading the Isotopic Code: American Geophysical Union Geophysical Monograph 95, p. 429–437, https://doi.org/10.1029/GM095p0429.

Vermeesch, P., 2018, IsoplotR: A free and open toolbox for geochronology: Geoscience Frontiers, v. 9, no. 5, p. 1479–1493, https://doi.org/10.1016/j.gsf.2018.04.001.

Wall, C.J., Scoates, J.S., and Weis, D., 2016, Zircon from the Anorthosite zone II of the Stillwater Complex as a U–Pb geochronological reference material for Archean rocks: Chemical Geology, v. 436, p. 54–71, https://doi.org/10.1016/j.chemgeo.2016.04.027.

Wall, C.J., Hanson, R.E., Schmitz, M., Price, J.D., Donovan, R.N., Boro, J.R., Eschberger, A.M., and Toews, C.E., 2021, Integrating zircon trace-element geochemistry and high-precision U-Pb zircon geochronology to resolve the timing and petrogenesis of the late Ediacaran–Cambrian Wichita igneous province, Southern Oklahoma Aulacogen, USA: Geology, v. 49, p. 268–272, https://doi.org/10.1130/G48140.1.

Wasserburg, G.J., Jacobsen, S.B., DePaolo, D.J., McCulloch, M.T., and Wen, T., 1981, Precise determination of Sm/Nd ratios, Sm and Nd isotopic abundances in standard solutions: Geochimica et Cosmochimica Acta, v. 45, no. 12, p. 2311–2323, https://doi.org/10.1016/0016-7037(81)90085-5.

Watson, E., Wark, D., and Thomas, J., 2006, Crystallization thermometers for zircon and rutile: Contributions to Mineralogy and Petrology, v. 151, no. 4, p. 413–433, https://doi.org/10.1007/s00410-006-0068-5.

Webster, R., 1959, Isotope dilution analysis, *in* Waldron, J.D., ed., Advances in Mass Spectrometry: Elsevier, p. 103–119, https://doi.org/10.1016/B978-0-08-009210-2.50013-4.

Wendt, I., 1984, A three-dimensional U/Pb discordia plane to evaluate samples with common lead of unknown isotopic composition: Chemical Geology, v. 46, no. 1, p. 1–12, https://doi.org/10.1016/0009-2541(84)90162-1.

Wendt, I., and Carl, C., 1991, The statistical distribution of the mean squared weighted deviation: Chemical Geology, v. 86, p. 275–285.

Wetherill, G.W., 1956, An interpretation of the Rhodesia and Witwatersrand age patterns: Geochimica et Cosmochimica Acta, v. 9, no. 5–6, p. 290–292, https://doi.org/10.1016/0016-7037(56)90029-1.

Weyer, S., Anbar, A.D., Gerdes, A., Gordon, G.W., Algeo, T.J., and Boyle, E.A., 2008, Natural fractionation of $^{238}U/^{235}U$: Geochimica et Cosmochimica Acta, v. 72, no. 2, p. 345–359, https://doi.org/10.1016/j.gca.2007.11.012.

White, L.F., Tait, K.T., Kamo, S.L., Moser, D.E., and Darling, J.R., 2020, Highly accurate dating of micrometre-scale baddeleyite domains through combined focused ion beam extraction and U–Pb thermal ionization mass spectrometry (FIB-TIMS): Geochronology, v. 2, no. 2, p. 177–186, https://doi.org/10.5194/gchron-2-177-2020.

Widmann, P., Davies, J., and Schaltegger, U., 2019, Calibrating chemical abrasion: Its effects on zircon crystal structure, chemical composition and U-Pb age: Chemical Geology, v. 511, p. 1–10, https://doi.org/10.1016/j.chemgeo.2019.02.026.

Wiedenbeck, M., Allé, P., Corfu, F., Griffin, W.L., Meier, M., Oberli, F., Von Quadt, A., Roddick, J.C., and Spiegel, W., 1995, Three natural zircon standards for U-Th-Pb, Lu-Hf, trace element and REE analyses: Geostandards Newsletter, v. 19, p. 1–23, https://doi.org/10.1111/j.1751-908X.1995.tb00147.x.

Wilkinson, M.D., Dumontier, M., Aalbersberg, I.J., Appleton, G., Axton, M., Baak, A., Blomberg, N., Boiten, J.-W., da Silva Santos, L.B., Bourne, P.E., Bouwman, J., Brookes, A.J., Clark, T., Crosas, M., Dillo, I., Dumon, O., Edmunds, S., Evelo, C.T., Finkers, R., Gonzalez-Beltran, A., Gray, A.J.G., Groth, P., Goble, C., Grethe, J.S., Heringa, J., 't Hoen, P.A.C., Hooft, R., Kuhn, T., Kok, R., Kok, J., Lusher, S.J., Martone, M.E., Mons, A., Packer, A.L., Persson, B., Rocca-Serra, P., Roos, M., van Schaik, R., Sansone, S.-A., Schultes, E., Sengstag, T., Slater, T., Strawn, G., Swertz, M.A., Thompson, M., van der Lei, J., van Mulligen, E., Velterop, J., Waagmeester, A., Wittenburg, P., Wolstencroft, K., Zhao, J., and Mons, B., 2016, The FAIR Guiding Principles for scientific data management and stewardship: Scientific Data, v. 3, no. 1, https://doi.org/10.1038/sdata.2016.18.

Williams, I.S., 1998, U-Th-Pb geochronology by ion microprobe, *in* McKibben, M.A., Shanks, W.C., III, and Ridley, W.I., eds., Applications of Microanalytical Techniques to Understanding Mineralizing Processes: Society of Economic Geologists Reviews in Economic Geology 7, p. 1–35, https://doi.org/10.5382/Rev.07.01.

Wotzlaw, J.-F., Schaltegger, U., Frick, D.A., Dungan, M.A., Gerdes, A., and Günther, D., 2013, Tracking the evolution of large-volume silicic magma reservoirs from assembly to supereruption: Geology, v. 41, p. 867–870, https://doi.org/10.1130/G34366.1.

Wotzlaw, J.-F., Hüsing, S.K., Hilgen, F.J., and Schaltegger, U., 2014, High-precision zircon U–Pb geochronology of astronomically dated volcanic ash beds from the Mediterranean Miocene: Earth and Planetary Science Letters, v. 407, p. 19–34, https://doi.org/10.1016/j.epsl.2014.09.025.

York, D., 1968, Least-squares fitting of a straight line with correlated errors: Earth and Planetary Science Letters, v. 5, p. 320–324, https://doi.org/10.1016/S0012-821X(68)80059-7.

York, D., Evensen, N.M., Lopez Martinez, M., and De Basabe Delgado, J., 2004, Unified equations for the slope, intercept, and standard errors of the best straight line: American Journal of Physics, v. 72, no. 3, p. 367–375, https://doi.org/10.1119/1.1632486.

Zheng, Y.-F., 1992, The three-dimensional U/Pb method: Generalized models and implications for U-Pb two-stage systematics: Chemical Geology, v. 100, p. 3–18, https://doi.org/10.1016/0009-2541(92)90099-Q.

Zhou, C., Huyskens, M.H., Lang, X., Xiao, S., and Yin, Q.-Z., 2019, Calibrating the terminations of Cryogenian global glaciations: Geology, v. 47, p. 251–254, https://doi.org/10.1130/G45719.1.

Science Editor: Brad Singer

Manuscript Received 8 September 2023
Revised Manuscript Received 9 January 2024
Manuscript Accepted 16 February 2024

Downloaded from http://pubs.geoscienceworld.org/gsa/gsabulletin/article-pdf/136/9-10/4233/6898541/b37321.1.pdf
by guest